TREBALL DE FI DE CARRERA

TÍTOL DEL TFC: Computational Fluid Dynamics study of 2D vertical axis turbines for application to wind and tidal energy production

TITULACIÓ: Enginyeria Tècnica Aeronàutica, especialitat Aeronavegació

AUTOR: Antonio Hernández Gómez

DIRECTOR: Adeline de Villardi de Montlaur

DATA: 13 de març de 2014

Título: Computational Fluid Dynamics study of 2D vertical axis turbines for application to wind and tidal energy production

Autor: Antonio Hernández Gómez

Director: Adeline de Villardi de Montlaur

Fecha: 13 de marzo de 2014

Resumen

Este proyecto consiste en el estudio de turbinas de eje vertical, las cuales a diferencia de las turbinas de eje horizontal clásicas tienen su eje de rotación perpendicular a la dirección del fluido (aire / agua). Entre las ventajas de este tipo de turbinas destaca la posibilidad de instalarlas en entornos urbanos gracias a su reducido tamaño. Así mismo las turbinas de eje vertical no necesitan un sistema de apuntamiento ya que pueden girar con independencia de la dirección del fluido, reduciéndose su coste de mantenimiento.

ANSYS Fluent se ha utilizado como software de Dinámica de Fluidos Computacional (CFD), para la realización de simulaciones con la suficiente precisión y fiabilidad en esta aproximación a las turbinas de eje vertical. El proyecto se inicia con una introducción a las turbinas, mostrando las principales diferencias entre las turbinas de eje horizontal y vertical. A continuación se detalla el proceso de configuración de Fluent, así como el desarrollo teórico que relaciona el coeficiente de potencia con el parámetro TSR (Tip Speed Ratio). Se ha procedido a la realización de un estudio de independencia del mallado y del muestreo temporal en Fluent, a fin de proceder a la validación de los resultados obtenidos.

Se han llevado a cabo varias simulaciones con el fin de obtener la configuración óptima de la turbina. Los parámetros de la turbina que han sido objeto de estudio han sido: cuerda de la pala, tipo de perfil aerodinámico, número de palas y el radio de la turbina. Las modificaciones realizadas sobre cada parámetro están enfocadas a la obtención de la máxima eficiencia de la turbina. Además, se presenta una comparación entre turbinas de viento y marinas. Finalmente se presentan las conclusiones y trabajo futuro que se podría realizar.

Title: Computational Fluid Dynamics study of 2D vertical axis turbines for application to wind and tidal energy production.

Author: Antonio Hernández Gómez

Director: Adeline de Villardi de Montlaur

Date: March, 13th 2014

Overview

This project consists in the study of vertical axis turbines, which in opposition to classical horizontal axis turbines have their axis of rotation perpendicular to the fluid (air/water) direction. These kinds of turbines have some advantages like their reduced size, allowing their installation in urban environments. Moreover, vertical axis turbines do not need a yaw pointing system, as they can rotate with independence of the fluid direction, which reduce their maintenance cost.

ANSYS Fluent has been used as Computational Fluid Dynamics (CFD) software, providing simulated results with enough accuracy and reliability into this approach to vertical axis turbines. The project begins with an introduction to turbines, showing the main differences between horizontal and vertical axis turbines. After that, the configuration process of Fluent is detailed, as well as the theoretical development that relates the power coefficient with the tip speed ratio of the turbine. A study about the validation of the results has been done, consisting in a mesh and time independence study.

Several simulations have been done in order to obtain the optimum configuration of the turbine. The turbine parameters that have been studied are: blade chord, airfoil type, number of blades and turbine radius. The modification of each parameter is aimed to obtain the maximum efficiency of the turbine. Furthermore, a comparison between wind and tidal turbines is described. Finally the conclusions and future work are presented.

Agradecimientos

Me gustaría agradecer a toda mi familia y amigos por el apoyo recibido durante la realización de este proyecto y en especial a mis padres y mi hermana Ana.

No me puedo olvidar de Livia, quien con su paciencia y comprensión ha sido un apoyo fundamental en esta aventura y sin la que este proyecto no habría podido salir adelante.

Por último agradezco a mi directora de proyecto Adeline por todos sus consejos y ayuda prestada en cada una de las etapas de este proyecto.

INDEX

LIST OF FIGURES

LIST OF TABLES

NOMENCLATURE

A	Reference area (m^2)
L	Reference length (m)
C_m	Moment coefficient
C_{mi}	Moment coefficient for blade *i*
$\overline{C_m}$	Averaged moment coefficient
c_p	Power coefficient
λ	Tip speed ratio
ρ	Density (kg/m^3)
M	Total moment generated by the turbine
R	Turbine radius (m)
ω	Angular velocity (rad/s)
v_∞	Free stream velocity (m/s)
P_a	Power available
P_t	Power extracted from the turbine
σ	Turbine solidity
Δt	Time step
$\Delta t\big\|_{1^o}$	Time step associated with 1 degree of rotation
θ	Angle of azimuth

INTRODUCTION

The main goal of this final thesis is to analyse different configurations of vertical axis turbines (VAT) and their application to energy production with the help of Ansys – Fluent. This Computational Fluid Dynamics (CFD) software is used to study the aerodynamic behaviour of different types of turbines, in order to optimize their efficiency. The use of CFD software is a powerful tool that allows obtaining simulated results that help in the design process of a real turbine.

The thesis is divided into 4 chapters. The first one is an introduction to vertical axis turbines and how they are able to extract energy from air and water to generate power. The axis of rotation of a vertical axis turbine is placed perpendicular to the fluid direction, giving this kind of turbine some advantages in front of horizontal axis turbines (HAT) as the capability to rotate independently of the wind direction without the use of a yaw pointing system. The chapter continues with a comparison between vertical and horizontal axis turbines, showing the main advantages and drawbacks of each type of turbine. Finally, a brief introduction to parameters involved in turbine efficiency such as the power coefficient and tip speed ratio is found.

In chapter 2 the configuration process of the vertical axis turbine in Ansys – Fluent is detailed. After the turbine geometry generation, the meshing process is described. From this point the setup of Fluent is detailed. The use of a sliding mesh technique to simulate the rotation of the turbine is explained, focusing on parameters such as the time step value used transient simulations like this. Finally the setup of the different boundary conditions is described.

The thesis continues with the third chapter, where some of the concepts that affect the results obtained in the simulations are detailed, as the meshing independence study and the choice of a proper time step value. Once the results have been validated, several simulations focused on different turbine parameters are presented. Therefore, the blade chord, airfoil type, number of blades and turbine radius and their effect over the turbine efficiency are studied. At the same time, a comparison between wind and tidal vertical axis turbines is presented. Finally, chapter 4 presents the conclusions and future work that could be done.

CHAPTER 1. VERTICAL AXIS TURBINES

1.1 Wind and tidal energy production

During the last decade renewable energy sources as sun, wind and ocean tides have been introduced step by step and have become more popular and used. Nowadays, the technology allows the construction of renewable power plants capable of generating great amounts of energy, and at the same time being non cost prohibitive. The global awareness on the need for environmental protection and the efforts to reduce greenhouse gas emissions put it clear that new energy models need to be developed.

1.1.1 Wind energy

Wind energy is nowadays one of the most economical and efficient energy renewable sources. This technology has proved to be mature enough to compete with other traditional energy sources such as thermal power plants.

In the last decade, there has been an extraordinary expansion in Spain in the use of wind energy for electricity generation. This has been possible because of the great number of potential locations that allow the installation of wind turbines, and the support policies that lead to a huge industrial and technological development in this sector. In December 2012 Spain had 22,785 MW of installed wind power capacity, being the fourth country in the world for wind energy production, only behind China, USA and Germany [1]. The growth of wind energy during the last 15 years as well as the cumulative capacity for the biggest country producers are detailed in figures **Fig. 1.1** and **Fig. 1.2**:

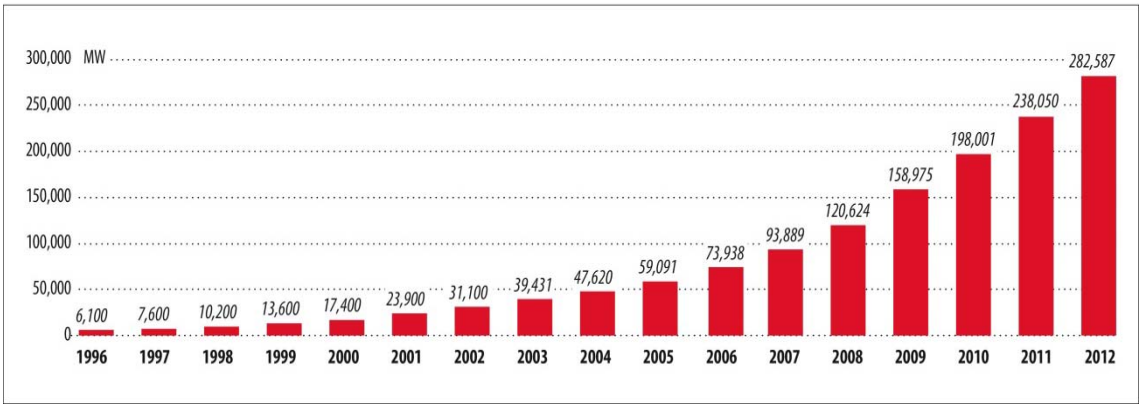

Fig. 1.1 Global Cumulative Installed Wind Capacity 1996-2012. [1]

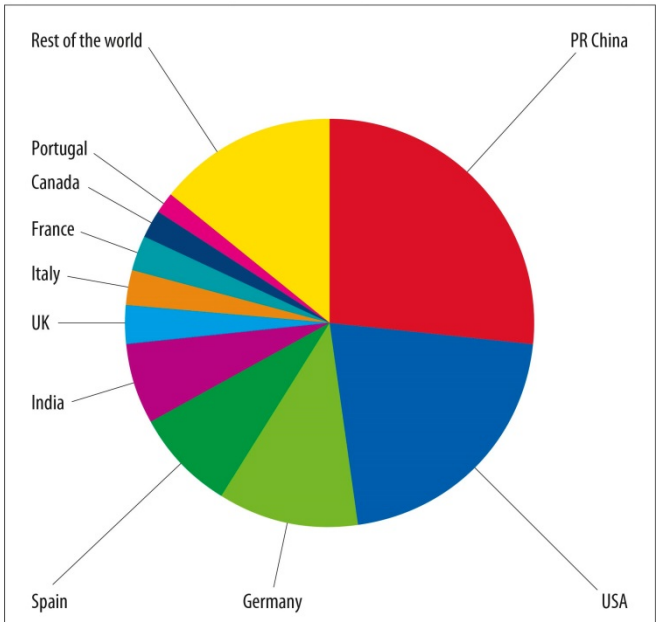

Country	MW	% SHARE
PR China	75,324	26.7
USA	60,007	21.2
Germany	31,308	11.1
Spain	22,796	8.1
India	18,421	6.5
UK	8,445	3.0
Italy	8,144	2.9
France	7,564	2.7
Canada	6,200	2.2
Portugal	4,525	1.6
Rest of the world	39,853	14.1
Total TOP 10	242,734	85.9
World Total	**282,587**	**100.0**

Fig. 1.2 Wind energy Top 10 Cumulative Capacity (December 2012). [1]

1.1.2 Tidal energy

Another form of renewable energy is the tidal energy, which exploits coastal tidal waters caused by the interaction of the gravitational fields of the Earth and moon. The tidal stream devices used to generate power are often quite similar to wind turbines, with some slight differences that occur due to the higher density of water compared with air. To increase the flow and power from the turbine, concentrators may be used around the blades to concentrate the flow towards the rotor.

The main advantages of this technology are: [2]

- Consistent Power – Tides move constantly throughout the day, which provides a consistent stream of electricity generation capacity and also are much more predictable than wind and solar energy.

- Low Operating Costs – Once installed there are few on-going operating costs or labour costs, unless there is a device breakdown.

- Minimal Visual Impact – Tidal power devices are fully or nearly completely submerged in water well offshore. This reduces the “damaging of water views” that has been associated with offshore wind turbines.

- Locations – There are numerous locations for tidal power around the world as the 70% of the earth’s surface is covered with water.

And its main drawbacks are:

- Device Breakdown – Strong ocean storms and salt water corrosion can damage the devices and cause frequent breakdowns, which increase the cost of the manufacturing process in order to have more durable devices.

- Marine Life Affected – Sea life can be harmed by the blades installed to generate power. The floor mounting could also disrupt the habitats of different sea life and plants.

- High Initial Costs – The high cost of the tidal stream generators, as well as the installation of power lines underwater, can lengthen the payback period, which might be not affordable depending on the characteristics and size of each project.

- Few Implemented – There are relatively few commercial installations compared to other technologies, such as wind and solar farms. Thus, additional difficulties implementing these installations could arise.

- Reduced Sea Usage – The potentially larger footprint of tidal power plants could reduce shipping and recreation areas.

It was previously commented that tidal current turbines operate on similar principles as wind turbines, taking into consideration that water is much denser than air. In addition, water flow speed is much lower than air.

$$\rho_{Water} = 1000 kg/m^3$$

$$\rho_{Air} = 1.225 kg/m^3$$

The bigger density implies that the loading forces and moments exerted on tidal turbines are higher than those that appear in wind turbines. So tidal current turbines must be able to generate electricity with tides and at the same time be able to withstand much higher structural loads even when they are not in use.

One of the key advantages of tidal current turbines versus wind turbines is that they can produce the same amount of power with a greatly reduced turbine size, which can be seen in figure **Fig. 1.3**. The reason of this is that the power available of a given flow is proportional to its density. Therefore, as water density is around 800 times bigger than air density, tidal turbines can generate the same amount of energy with a reduced size compared to air turbines. The expression of power is detailed in equation **(1.2)**

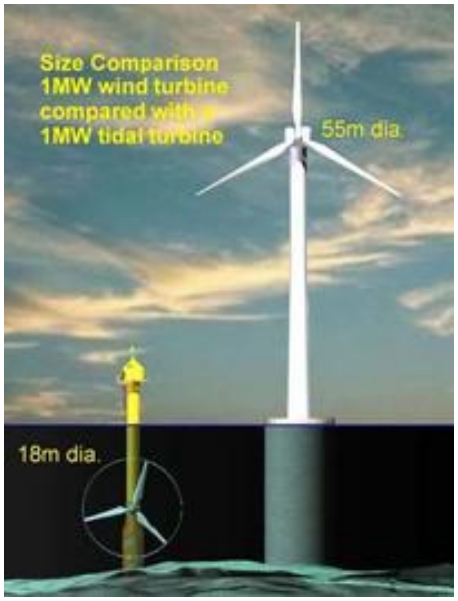

Fig. 1.3 Size comparison of tidal turbine vs. wind turbine [3]

1.2 Turbines considerations

In order to produce energy or electricity from wind or water movement, a turbine is used to extract energy from the fluid kinetic energy using its blades attached to a shaft. Before introducing the CFD simulations, which are the core of this thesis, a brief comparison between vertical and horizontal axis turbines is shown in this section.

1.2.1 Rotor axis orientation

According to the rotor axis orientation in relation with the flow direction, turbines are classified into horizontal axis turbine (HAT) and verticals axis turbines (VAT).

- Horizontal Axis Turbines (HAT): The rotational axis is parallel to the fluid direction. These kinds of turbines provide greater efficiency than VATs and, because of that, currently most of the wind turbines used in power plants are of this type. On the other hand, they require a larger area or location to be installed, making them profitable only in areas where permanent winds and high speeds are available. Furthermore, rotor blades need to face directly to wind or water direction in order to work properly.

- Vertical Axis Turbines (VAT): In these turbines the rotational axis is oriented perpendicular to the fluid direction. One of their main advantages is that they can rotate independently of the fluid direction, which implies that there is no need of using a yaw pointing system [4]. Another important benefit of VATs is that their production is much simpler than HAT's due to the constant cross-sections blades.

  Besides, VATs can be installed on the ground or house roofs so they become much more accessible than HATs. They are easier to repair and the maintenance cost is lower. As they are smaller, they are more suitable for urban environments, where they can be used to increase the electrical power generation capacity, where the size and noise emissions limitations prohibit the use of HATs. In this kind of environment, VATs take profit of the rapidly changing conditions like wind direction and wind speed, whereas HATs need a constant speed as well as a predominant wind direction to work efficiently.

Horizontal Axis Wind Turbine [5]

Vertical Axis Wind Turbine [6]

Fig. 1.4 HAWT and VAWT

1.2.2 Tip Speed Ratio

The Tip Speed Ratio (TSR) or λ is a parameter that relates the rotational velocity of the turbine and the free stream velocity with the expression given below:

$$\lambda = \frac{\omega R}{v_\infty} \tag{1.1}$$

Where:

R = Radius of the turbine.
ω = Rotational velocity of the turbine.
v_∞ = Free stream wind velocity.

This expression is very important in turbines, as normally the efficiency of the turbine is plotted as a graph showing the power coefficient as a function of the tip speed ratio. The power coefficient C_p is the amount of power that the turbine is able to extract from the flow (wind or water). First, the power available from the wind, and the power extracted from the turbine need to be calculated as:

$$P_a = \frac{1}{2}\rho A v_\infty^3 \tag{1.2}$$

$$P_t = M\omega \tag{1.3}$$

Where:

P_a = Power available from the wind.
P_t = Power extracted from the turbine.
M = Total moment generated by the turbine.
A = Turbine frontal area.

Then, using the previous expressions, the power coefficient can be calculated as:

$$C_p = \frac{P_t}{P_a} = \frac{M\omega}{\frac{1}{2}\rho A v^3} \tag{1.4}$$

It is always desirable to work near the zone where the power coefficient reaches its maximum, in order to extract the maximum power from the turbine. As we

move to tip speed ratios far from the optimum value, the efficiency of the turbine will decay. Moreover, with high values of the tip speed ratio some undesirable effects may arise, as higher loads and noise level due to large centrifugal forces. To deal with that, the turbine structure and the blades must be strong. Working with variable velocity rotor turbines allows achieving an optimum performance, as they change their rotational velocity as a function of the air velocity in order to work near the optimum tip speed ratio.

German physicist Albert Betz demonstrated, applying the principles of conservation of mass and momentum of the air stream, that the maximum efficiency of a turbine is 16/27 (0.59), which is known as the Betz's limit. A more detailed description is given in [7]. It is important to remark that the Betz's limit cannot be achieved because other non-ideal effects appear in real turbines, lowering the overall efficiency.

The figure **Fig. 1.5** shows the efficiency for different kinds of wind turbines:

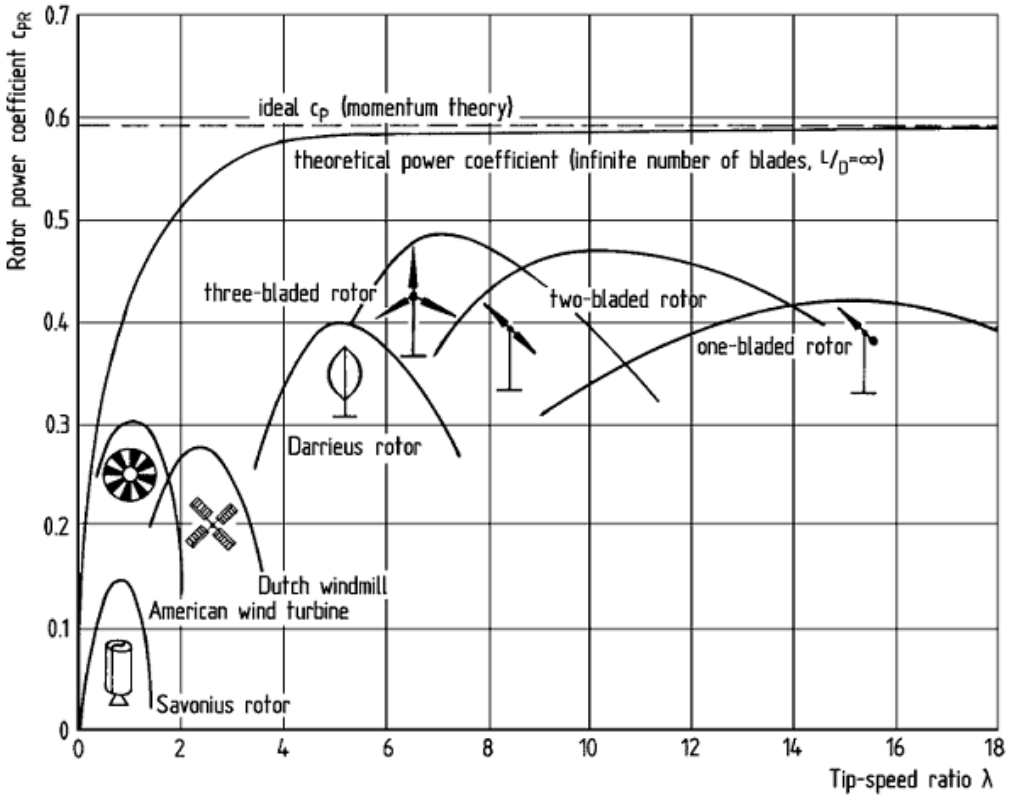

Fig. 1.5 Cp vs λ for different types of wind turbines [8]

CHAPTER 2. CFD SIMULATION ENVIRONMENT

This thesis main objective is to explain the effect of the variation of some basic turbine parameters, as chord length and shape, over the performance of a vertical axis turbine through CFD simulations. In this chapter, the main principles of a CFD simulation, moving from the generation of the turbine geometry and the meshing of the model to the Fluent configuration setup are presented

The flow chart shown in figure **Fig. 2.1** details the process applied in this thesis to obtain the results presented in chapter 3 using the *Ansys – Fluent* application.

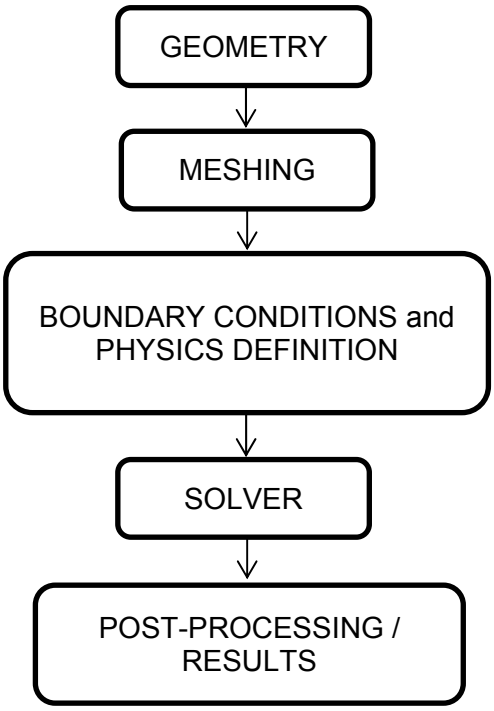

Fig. 2.1 CFD Simulation Flow Chart [9].

2.1 Turbine Geometry

The geometry of the different turbines used in the simulations was generated using *Ansys Design Modeller*. It was not feasible to simulate a 3D turbine due to computational cost, so all the simulations carried out consisted of 2D turbines. In order to generate the turbine geometry with *Ansys Design Modeller*, a file containing the coordinates of the airfoil from the leading edge to the trailing edge was obtained from [10]. These airfoils will be the blades of the turbine which are the main component when designing a turbine. The next step is to read the file containing the airfoil coordinates, and then generate the final turbine geometry using different options such as resizing, translate and scale.

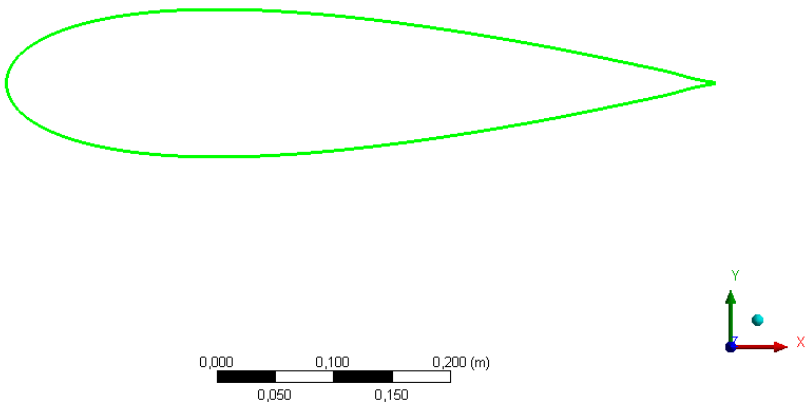

Fig. 2.2 NACA 0021 airfoil geometry in *Ansys Design Modeller*.

The airfoils used in the simulations belong to the 4-digit NACA series which are defined by [11] [12]:

- The first digit describes maximum camber as a percentage of the chord airfoil.
- The second digit describes the distance where maximum camber of the airfoil is reached from the leading edge in tens of percents of the chord.
- The last two-digits describe the maximum thickness as percentage of the chord airfoil.

For any symmetrical airfoil, the first two digits are 00 indicating that the airfoil is not cambered [13]. Symmetrical NACA airfoils have been used in the simulations as it was pointed in most of the references as a good choice for vertical axis turbines [14]. Moreover, the use of symmetrical airfoils eases the manufacturing process of the turbine and its costs, which are two important factors as explained in chapter 1 that can help broadening the use of these turbines.

For simplicity of the design, the central shaft and the blades supporting arms of the turbine have not been considered in the simulations. Finally, in order to simplify the results acquisition using the *Fluent* application, all the geometries generated consider the centre of the turbine as the origin of the main coordinate system. In figure **Fig. 2.3** the geometry of a four bladed vertical axis turbine is shown:

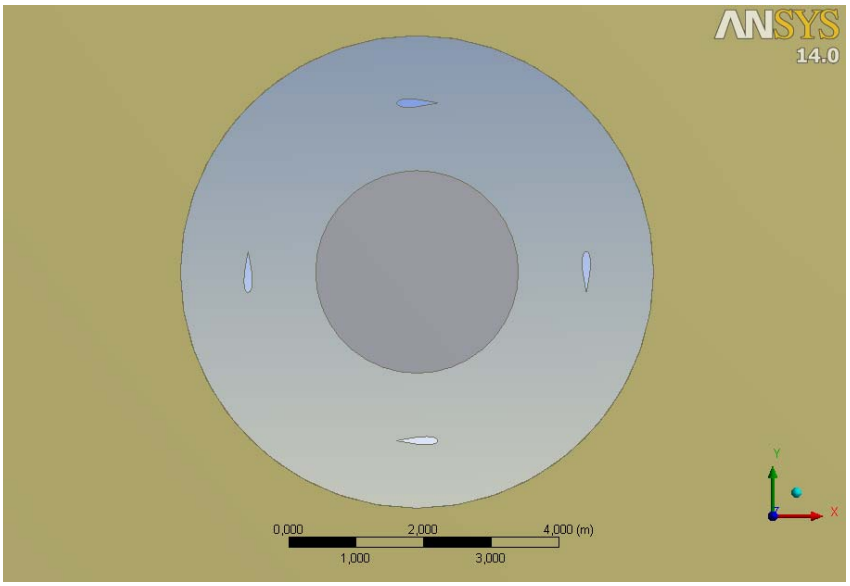

Fig. 2.3 Geometry of a four bladed vertical axis turbine. Radius = 2.5 m.

2.2 Mesh domain

After the geometry generation process, the next step in CFD simulations is the discretization of the entire flow domain, which is divided in small cells using tetrahedrals where the Navier-Stokes equations will be solved. This process is named “grid generation” and is one of the most important parts of a CFD simulation. A compromise between grid density and computational cost has to be done, because a poor density grid will lead us to solutions far away from the reality. Refining the mesh provides more accurate information up to a certain point where, as the number of cells increases, there is no significant change in the parameters of interest of our model. This step is explained in detail in section 3.1 (Mesh Independence study).

A ‘C-shape’ domain around the turbine is generated to simulate the zone of interest of the fluid. The blades of the turbine are placed inside a rotating ‘O-shape’ domain simulating the movement of the turbine, while the rest of the fluid remains in a fixed domain.

Attention must be paid when choosing the dimensions of the simulation domain, so that all the fluid effects, like the wake turbulence for example, could be developed properly. The size domain has been increased progressively until simulation errors, like the reverse flow due to the small distance between the walls, disappeared. The figure **Fig. 2.4** shows the domain zones defined in *Fluent*, as well as the size of the simulation domain.

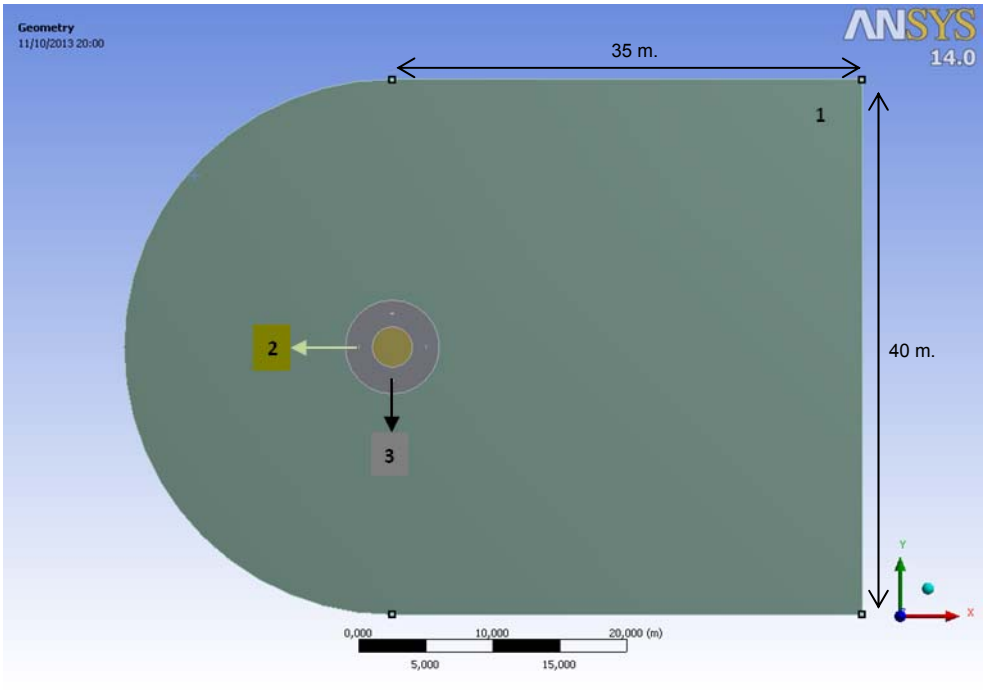

1. Stationary outer cell zone.
2. Stationary inner zone.
3. Rotating cell zone (sliding mesh).

Fig. 2.4 Simulation cell zones for a vertical axis turbine. Radius = 2.5 m.

To simulate the rotation of the turbine a sliding mesh technique has been used [15]. This kind of simulation consists of a part of the mesh changing with time accordingly to the rotational velocity desired in each simulation. Therefore, a transient simulation is used in *Fluent* with a time step chosen to rotate the mesh. The rotating and fixed domains are linked together using an interface, which ensures that the flow properties are passed correctly between cells placed in different domains.

The zone where the fluid interacts with the blades must be simulated precisely, as this zone has a great impact in the overall turbine performance results. So, in order to detect the high pressure and velocity gradients that appear near the airfoils of the turbine, a higher mesh density is needed in the rotating zone. **Fig. 2.5** and **Fig. 2.6** state perfectly clear that the mesh density is higher in the rotating zone than in the rest of the grid.

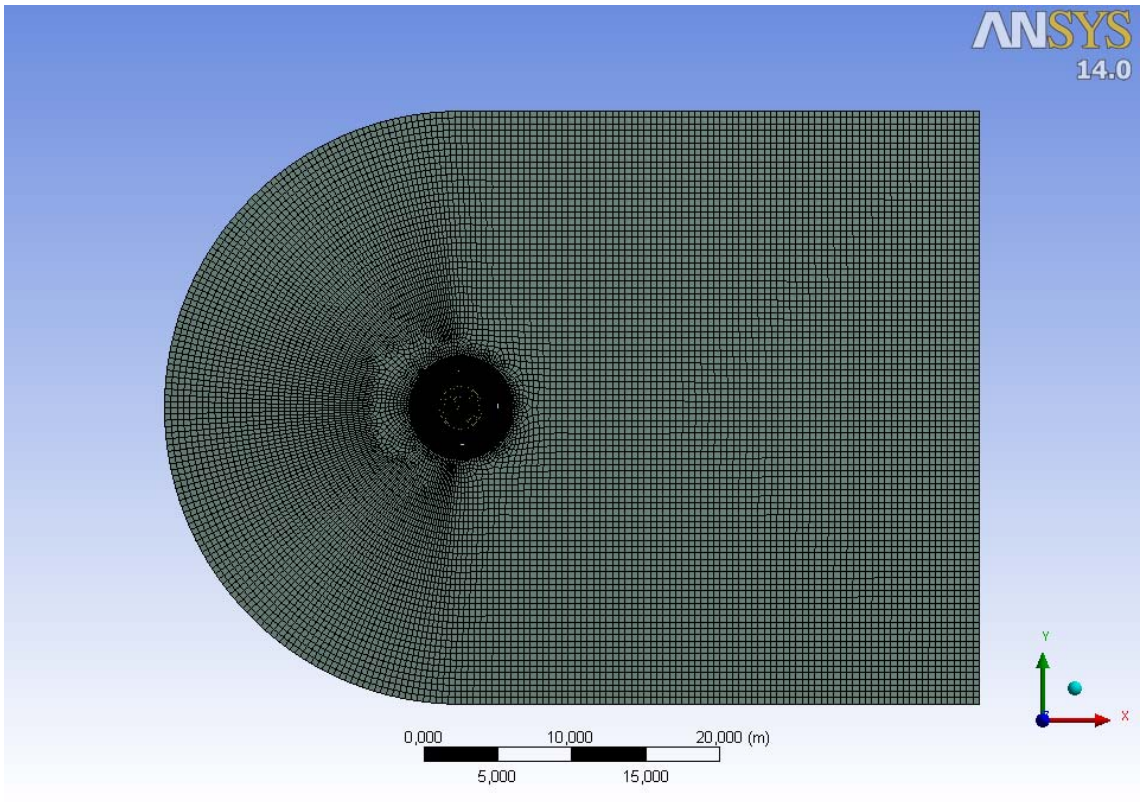

Fig. 2.5 Mesh grid.

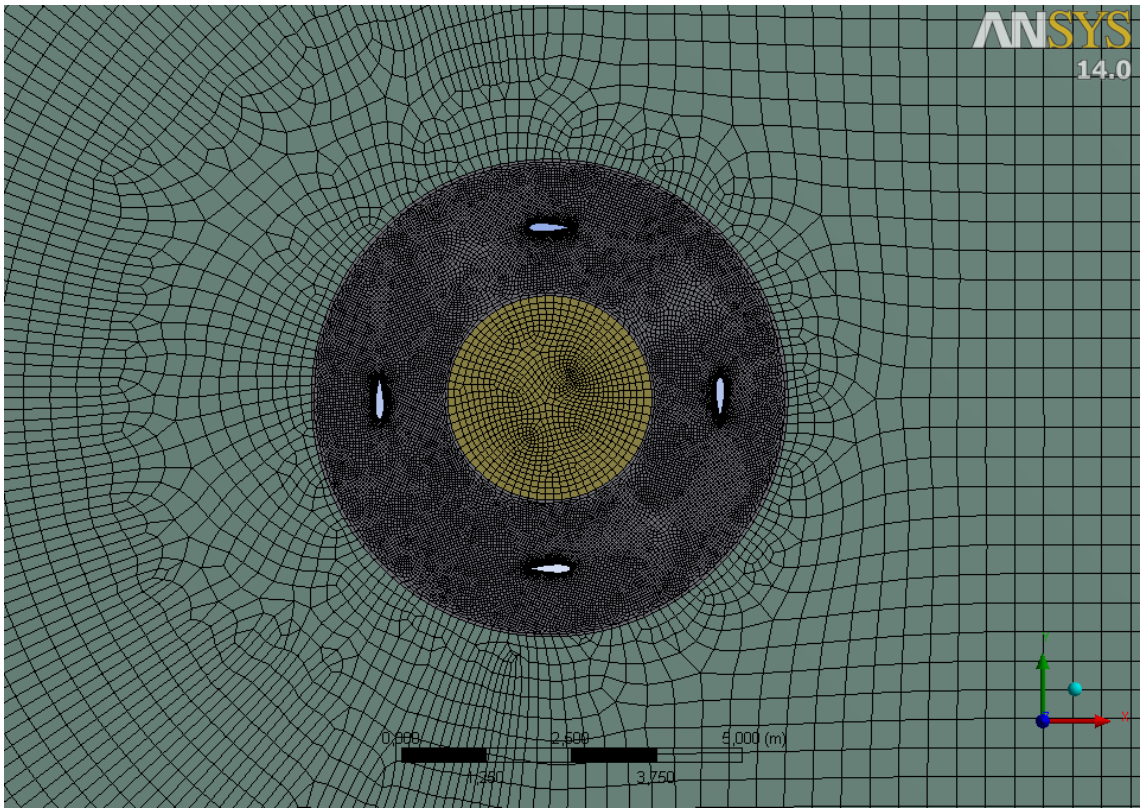

Fig. 2.6 Finer mesh around the blades.

2.3 Simulation Model – Setup

This section deals with the configuration and setup of *Fluent* application used in the simulations of this thesis, the choice of the numerical solver and the selection of the turbulence model among other options.

A pressure-based solver is used as *Fluent* user guide recommends it when solving incompressible flows [16]. At the same time, because of the unsteady behaviour of the flow, a time-dependent solution is required [17]. Therefore, during the calculation, the rotating mesh slides relative to the stationary one in discrete steps depending on the time step value.

2.3.1 Boundary conditions

Once the geometry and the mesh are generated, the next step in the simulation process is the definition of the boundary conditions of the system. These boundary conditions are shown in figure **Fig. 2.7**, and consist of a velocity inlet on the left side that simulates the air flow and a pressure outlet on the right side. The direction of the inlet velocity is forced to be parallel to the x-axis, while its magnitude depends on the fluid used. A nominal value of 10 m/s has been used for air simulations. This value has been reduced to 1 m/s when simulating tidal turbines [18] [14].

V_∞ (inlet)	
Air	Water
10 m/s	1 m/s

Table 2.1 Free stream flow velocities.

There are also two walls on the top and bottom part of the simulation area in which the no-slip condition is enforced. The combination of velocity inlet and pressure outlet boundary conditions is recommended by *Fluent* [16] when working with incompressible flows, as it happens in this thesis where the Mach number is very far away from values where compressible effects might appear.

It is necessary to select boundary conditions properly in *Fluent*, as they are key factors in order to achieve a realistic solution. Therefore, the physical phenomena that apply to our simulation must be studied carefully prior to define the boundary conditions of the simulation model.

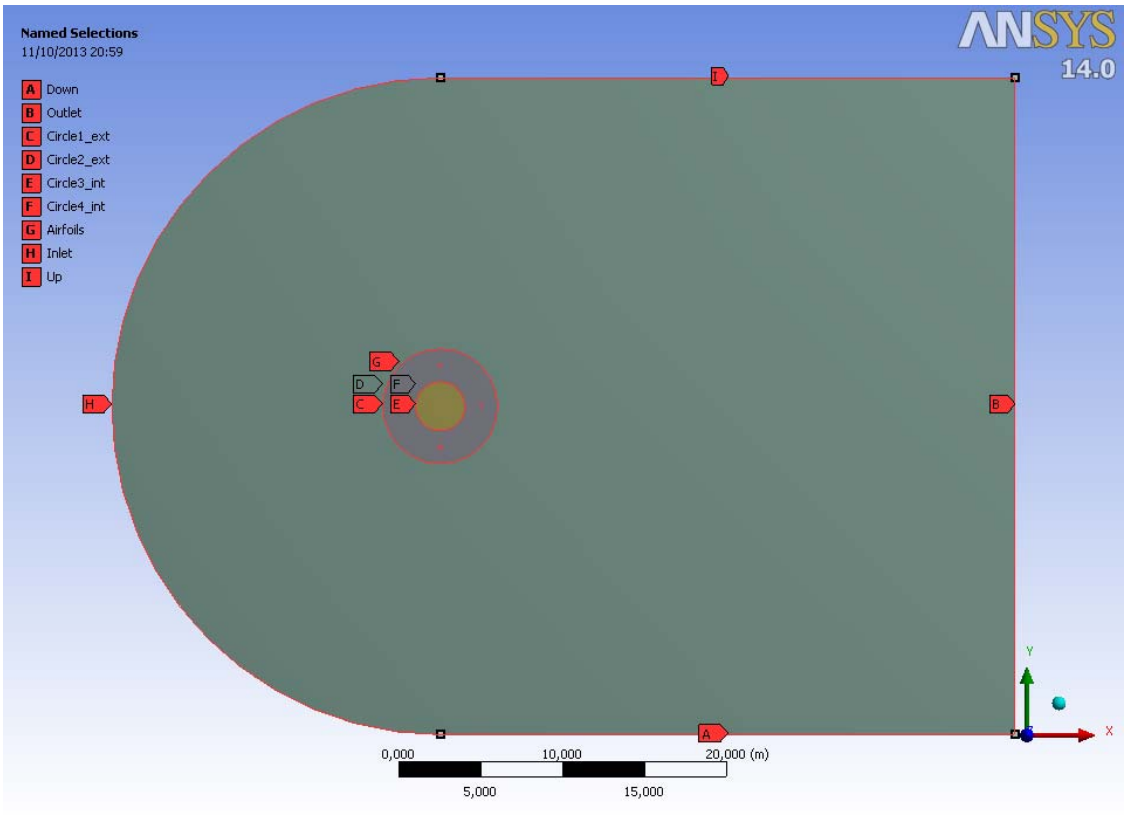

Fig. 2.7 Named Selections for Boundary Conditions.

The blades of the turbine are placed in a rotating domain. As explained before, in order to separate the stationary and the rotating domains, it is necessary to create an interface. In the simulations there are two transitions between rotating and stationary domains, so two different interfaces have to be created. They are created using the named selections '*Circle*'. It is important to remark that each interface links two different cell zones, being this the reason to create 2 named selections in each cell zone for every interface.

The interface definition process is a very important step during *Fluent* setup and a wrong definition will lead to non-realistic results. This happened during the first simulations where the value of the average moment coefficient obtained was negative for every range of tip speed ratio values simulated. As recommended by [17], the mass flow quantity was studied at both sides of the cell zones separated by an interface. Because of the continuity equation [12], this parameter has to be the same at both sides. The mismatch that was found made clear that that there was a problem between the interfaces, and that the information was not passed properly between the cells belonging to different cell zones. The interfaces were deleted and generated again to solve that problem.

2.3.2 Turbulence model

Fluent allows the use of different turbulence models depending on the nature of the problem to be studied. In this case, as in most of the references found about vertical axis turbines, the Shear Stress Transport (SST) was used. SST turbulence model is a 4-equation model based on a combination of the 2-equation models k-ε and k-ω. According to [19], SST gives better results for the type of flows expected in vertical axis turbines. *Fluent* default values have not been modified.

2.3.3 Time step calculation

As it was previously explained, a transient simulation requires the use of time-dependent calculations. In the case of a sliding mesh problem, this time step sets up, accordingly with the enforced rotational velocity of the turbine, the amount of degrees that the mesh rotates in every calculation. Instead of working with the value of the time step, the relation between the degrees of rotation of the sliding mesh per time step was used, as it proved to be an easier and more comprehensive parameter to work with. In the next lines the relation between these two parameters is described:

The process starts setting the rotational velocity of the turbine ω. The next step consists in calculating the time-step required to rotate one degree, taking into account the relation between radians and degrees:

$$\omega = \frac{\Delta\varphi}{\Delta t} \tag{2.1}$$

$$\Delta t = \frac{\Delta\varphi}{\omega} \tag{2.2}$$

$$\Delta t\big|_{1^\circ} = \frac{1}{\omega(rps).360} \tag{2.3}$$

It is important to notice from the previous equation the relation between the time step and the rotational velocity. This implies that for the whole range of tip speed ratio values from which we want to obtain the turbine performance, the time step must be changed accordingly. In **Table 2.2** appear some values of tip speed ratio and their time step value for a 5 meter diameter VAWT and a free stream velocity equal to 10 m/s.

TSR	ω (rad/s)	ω (rpm)	Δt_{1° (ms)
1	4	38.20	4.36
1.5	6	57.30	2.91
2	8	76.39	2.18
2.5	10	95.49	1.75
3	12	114.59	1.45
3.5	14	133.69	1.25
4	16	152.79	1.09

Table 2.2 VAWT - Time step values - v_∞=10 m/s – Diameter = 5m.

In chapter 3, a time independence study details the process to decide a proper time step value.

2.3.4 Reference values and power coefficient

Fluent allows setting the reference quantities used for computing normalized flow field variables as lift, drag and moment. In chapter 1, the expression of the power coefficient C_p was detailed in equation **(1.4)**: [20]

$$C_p = \frac{P_t}{P_a} = \frac{M\omega}{\frac{1}{2}\rho A v^3} \qquad \textbf{(2.4)}$$

In *Fluent*, the value of the total moment *M* is obtained using the moment coefficient C_m defined as:

$$C_m = \frac{M}{\frac{1}{2}\rho v^2 AL} \qquad \textbf{(2.5)}$$

In the previous equation, *A* is the reference area and *L* is the reference length. Taking into account these previous considerations, the expression of the power coefficient can be reduced as follows:

$$C_p = \frac{M\omega}{\frac{1}{2}\rho A v^3} \qquad \textbf{(2.6)}$$

$$C_p = \frac{C_m \frac{1}{2}\rho v^2 AL\omega}{\frac{1}{2}\rho A v^3} = C_m \frac{\omega L}{v} \quad \textbf{(2.7)}$$

When dealing with turbines in 2D simulations, the value of *A* is equal to the diameter of the turbine whereas the value of *L* is equal to the radius of the turbine as detailed in [21]. Applying these changes to the equation **(2.7)** results:

$$C_p = C_m \frac{\omega R}{v} \quad \textbf{(2.8)}$$

Finally, using the definition of the tip speed ratio from equation **(1.1)** in equation **(2.8)** allows us to obtain a simple expression that relates the power coefficient with the tip speed ratio and the moment coefficient extracted from *Fluent* simulations:

$$C_p = C_m \lambda \quad \textbf{(2.9)}$$

Apart from this geometric reference values which only depend on the size of the turbine, there are other kind of parameters as density and viscosity related with the fluid type. In the simulations, all the reference values have been computed from the inlet boundary condition, which forces the value of the free stream velocity. In **Table 2.3** the main reference values used in the VAWT and VATT simulations are detailed. These values may be set either manually or automatically by the *Fluent* materials database once the fluid is defined in the *Materials* dialog box in the *Problem Setup* menu.

Parameter	Air (VAWT)	Water (VATT)
Density (kg/m^3)	1.225	998.199
Viscosity (kg/m-s)	1.7894e-5	1.003e-3
Velocity (m/s)	10	1
Area (m^2)	Turbine Diameter	
Length (m)	Turbine Radius	

Table 2.3 VAWT and VATT Fluent reference values.

2.3.5 Solution methods

Several *Fluent* solver algorithms have been tested with almost no significant difference in the simulated parameters as the moment coefficient. However, using the main guidelines given in *Fluent Theory Guide* [22] the *PISO* Pressure-Velocity Coupling scheme has been chosen as Fluent recommends its use for transient or unsteady simulations.

The next step in *Fluent* is to select the Spatial Discretization methods:

- Gradient: The *Fluent Theory Guide* recommends the use of the *Least Squares Cell Based* for unstructured meshes.
- Pressure: *PRESTO!* method is used for transient simulations.
- Momentum: *Second Order Upwind* is used for higher accuracy instead of the *First Order Upwind* that may provide a faster convergence.

The rest of the parameters are set by default as given in Fluent.

CHAPTER 3. RESULTS AND DISCUSSIONS

After detailing the configuration process of Fluent, this chapter presents the results obtained in the simulations that have been carried out. In these simulations different geometric parameters of the turbine as the blade chord, turbine radius and blade shape were modified in order to study their impact in the global efficiency of the turbine. Moreover, a comparative study between tidal and wind vertical axis turbines can be found. In addition, different considerations regarding the simulations are explained, so that the results obtained could be validated.

First of all a discussion about the size of the mesh is presented, which is usually known as a mesh independence study, and is a key factor in CFD simulations. In parallel, a time step independence study is conducted as it was introduced section 2.3.3.

3.1 Mesh Independence study

When working with CFD the meshing becomes one of the most important processes in our study. This could lead us to think that the finer the mesh the better the results obtained, which is generally true. Although it must be taken into account that, as we reduce the size of the cell elements of our mesh, the simulation time to reach a final solution increases. Because of that, there has to be some kind of trade-off between the precision of the results and the computational cost of the simulation.

In order to validate the results obtained in the simulations a mesh independence study must be done previously. This kind of study starts with a given mesh designed to our specific problem, and consists in the evaluation of a variable of interest of our model as the mesh gets finer. As the cell size is reduced providing a finer mesh, the results obtained are more precise than the ones obtained with a coarser mesh. This process is iterated until the difference between the results obtained is lower than the desired tolerance of error. At this moment it can be said that the convergence of the results has been reached from the mesh point of view. From this point on, there is no need to continue reducing the size of the cell elements, as there would be no difference in using a finer mesh apart from an increase in the calculation time.

In this study an initial mesh was designed while the size of its elements was reduced progressively according to a factor called *Mesh Factor.* The Mesh Factor values used were: 0.85, 0.7, 0.6 and 0.5. As it can be seen in **Fig. 3.1** and **Table 3.1**, there is almost no difference in the value of the power coefficient calculated using a Mesh Factor value of 0.5, 0.6 and 0.7. Therefore, we can conclude that working with the mesh of Mesh Factor equal to 0.7 is enough, as refining more the mesh does not change substantially the results obtained, and would only increase the computational time of the simulations. This mesh is formed approximately by a number of 40,000 cells.

Mesh Factor	Cp
1	0.385
0.85	0.369
0.7	0.412
0.6	0.413
0.5	0.412

Table 3.1 Values of the power coefficient.

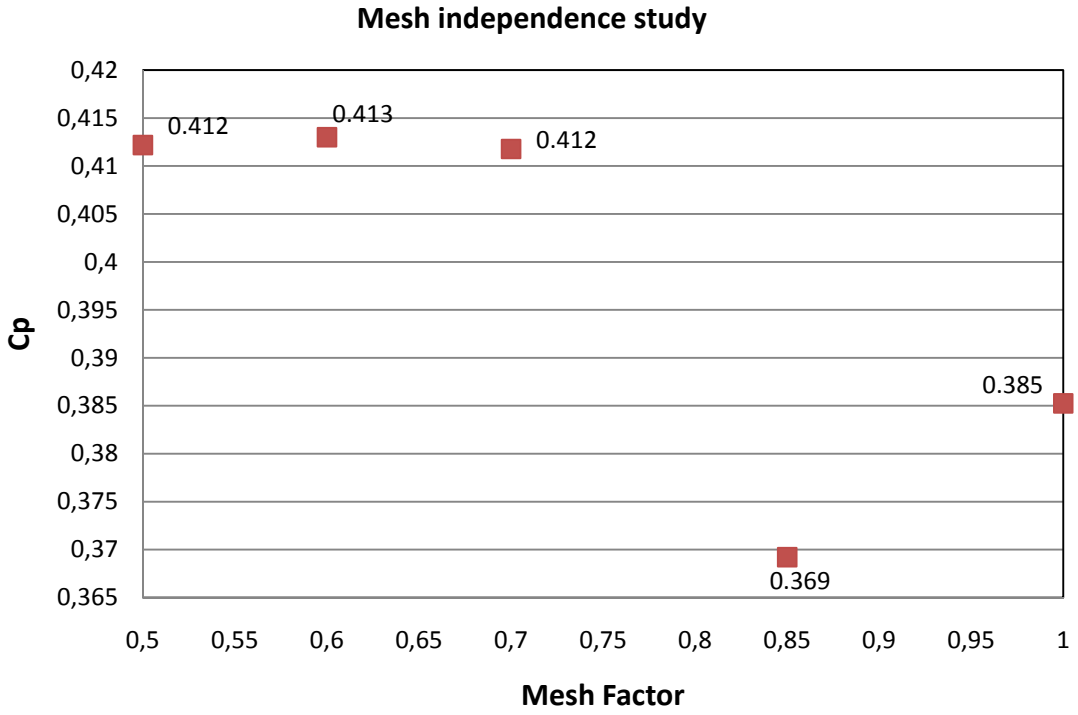

Fig. 3.1 Power coefficient as a function of the Mesh Factor.

3.2 Time step independence study

As it was introduced in section 2.3.3 regarding the time step calculation, and in order to validate the results of the simulations, several tests were done prior to choose the time step value. A high time step value is associated with a high displacement of the mesh, which could lead to a non-converging solution. On the other hand if the value of the time step is too low the convergence of the solution is ensured but the simulation time increases with no significant change in the solution. Therefore, a compromise has to be reached between the total simulation time and the maximum time step value.

Different time steps were tested over a VAWT so that their influence in the results could be evaluated. With a constant value of 2 for the tip speed ratio, the simulations consisted in measuring the value of the average moment coefficient of the turbine over a complete revolution as the time step value was increased. In order to have a better understanding of the problem, the angle of rotation of the mesh per time step was used, instead of working directly with the time step value.

Table 3.2 presents the results considering for the relative error the 1º time step as the reference value.

Rotation/time step	Averaged Cm	Relative error (%)
1º	1.356	-
3º	1.332	1.777
5º	1.383	1.991

Table 3.2 Cm error as a function of the time step.

A maximum relative error for the coefficient moment of 1.9% is achieved with a 5º rotation per time step. This error is considered low enough and allows validating the 5º mesh rotation per time step as the default value for all the simulations. A 4º mesh rotation per time step was used in [23] providing good results.

3.3 Simulations

In this section, and after validating the mesh and the time step value, the results obtained in the simulations are presented. When the setup of *Fluent* is completed as explained in the previous chapter, the simulation is started.

Fluent allows obtaining the instantaneous value of the moment coefficient for each blade of the turbine. However, as we are interested in the global efficiency of the turbine, working with the total moment coefficient is enough. The total moment coefficient is the sum of the moment coefficient for each blade. Therefore, for a N-bladed turbine the value of the turbine moment coefficient (C_m) is:

$$C_m = \sum_{i}^{N} C_{m_i} \qquad \textbf{(3.1)}$$

Next figure presents an example of the total moment coefficient for a turbine, where two different behaviours are shown: first of all, an initial transient state, and after the solution is converged, a steady state with a periodic pattern repeating for every complete rotation of the turbine.

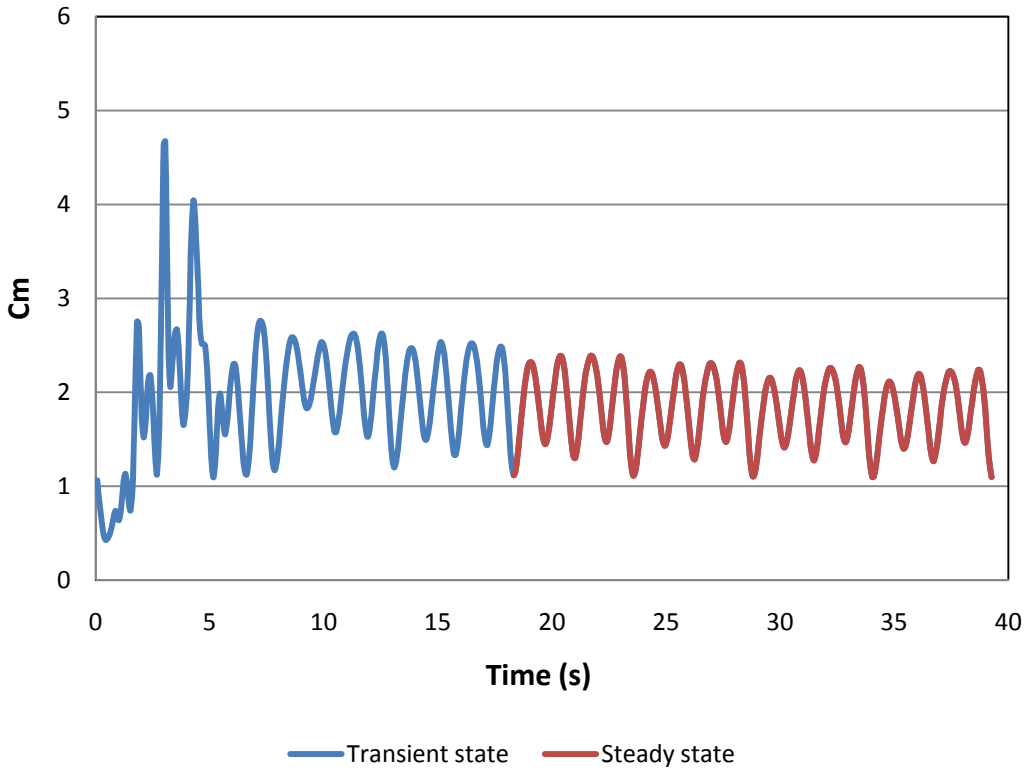

Fig. 3.2 Moment coefficient as a function of time.

In order to obtain the efficiency of the turbine, the different values of the steady state are averaged. In this average process the transient effect must not be taken into account, therefore the part of the graph in blue is discarded.

$$\overline{C_m} = \frac{\sum_t C_m}{\#\,samples} \qquad \textbf{(3.2)}$$

Once the averaged moment coefficient is obtained, the efficiency of the turbine is calculated as explained in equation **(2.9)**. **Fig. 3.3** shows the main reference system used in this thesis, considering a four bladed turbine. The angle formed between the x-axis and the line joining the blade position with the origin of the coordinate system is defined as the azimuth angle (θ).

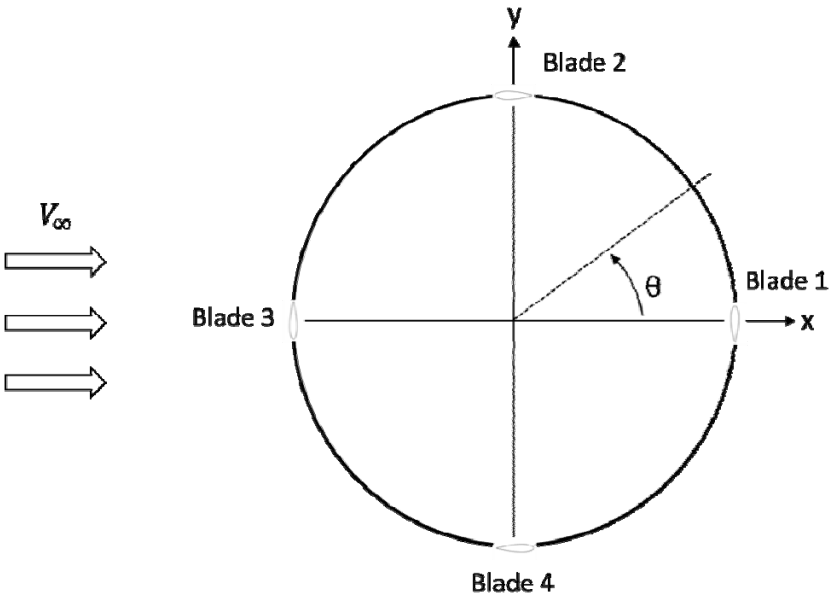

Fig. 3.3 Coordinate system.

3.3.1 Comparison of Wind and Tidal Turbines

The main purpose of these simulations is to study the differences between wind and tidal turbines. Therefore, the simulations consisted in placing the same turbine in water and air with their different fluid conditions: density, viscosity and the free stream velocity as it was detailed in **Table 2.3**. The Reynolds number (Re) was calculated for every type of turbine using equation **(3.3)**. Reynolds number is used when comparing different flows as occurs in this case, apart from characterizing different flow regimes [12].

$$\mathrm{Re} = \frac{\rho v c}{\mu} \qquad \textbf{(3.3)}$$

Table 3.3 shows the value of the Reynolds number as a function of the chord length and the optimum tip speed ratio values for each turbine:

	Air (VAWT)	**Water (VATT)**
Re/c	7.10^5	10.10^5
λ_{opt}	2.5	3

Table 3.3 Reynolds number for VAWT and VATT.
Radius = 2.5 m. -Chord = 0.6 m. – NACA0012.

Values of velocity are shown in **Fig. 3.4** and **Fig. 3.5** for the blades near the maximum moment position (θ=180º). These figures were obtained considering the optimum tip speed ratio for each turbine. Apart from the obvious difference

regarding the fluid velocity, the comparison of the two figures shows that there is no major difference in the distribution of velocity around the airfoil for air and water. The fact that the Reynolds numbers for both turbines are in the same order of magnitude lead to these results. In addition, the tip speed ratio values used in the comparison are similar as it can be seen in **Table 3.3** and **Fig. 3.9**. Similar effects were observed in [14]

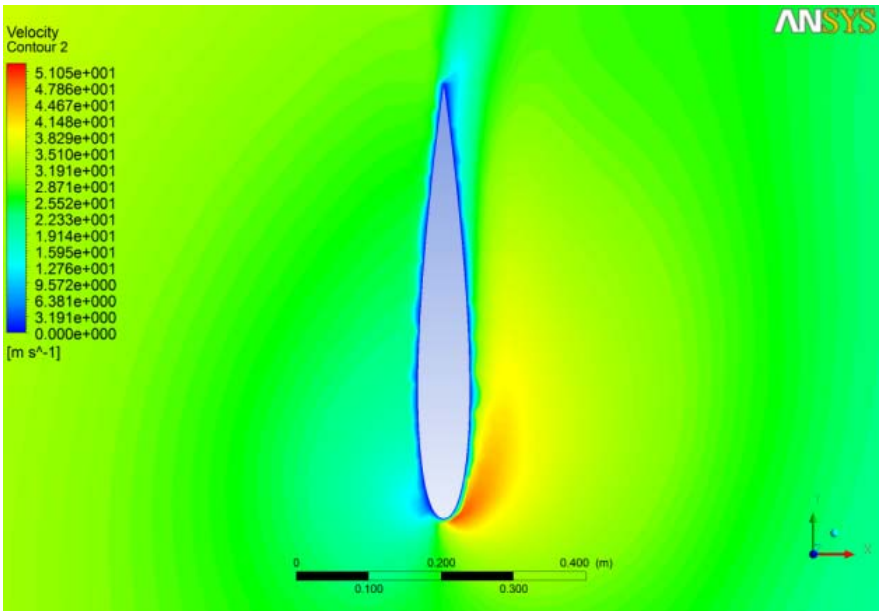

Fig. 3.4 VAWT - Velocity for the blade located at θ=180º. Radius = 2.5 m. -Chord = 0.6 m. – NACA0012.

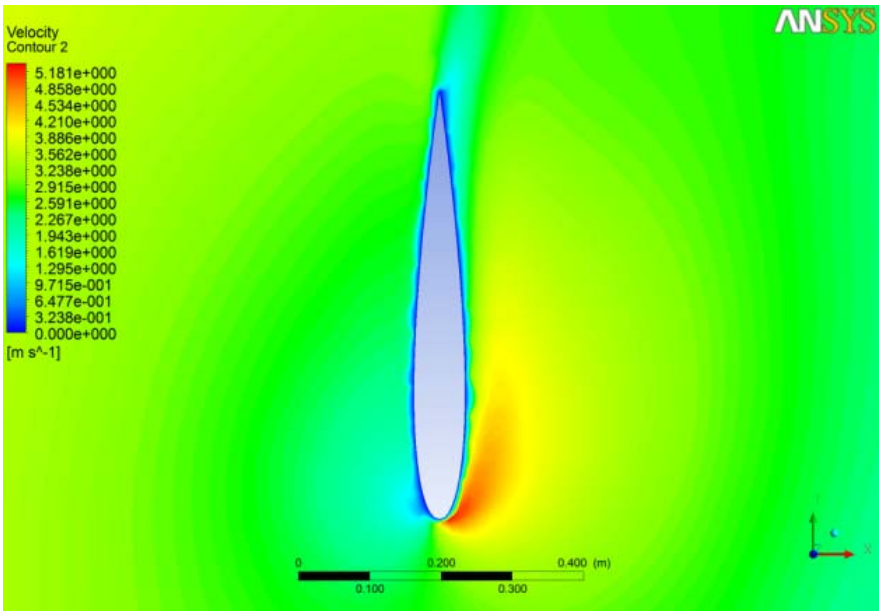

Fig. 3.5 VATT - Velocity for the blade located at θ=180º. Radius = 2.5 m. -Chord = 0.6 m. – NACA0012.

At the same time a pressure distribution study is presented in **Fig. 3.6** and **Fig. 3.7**

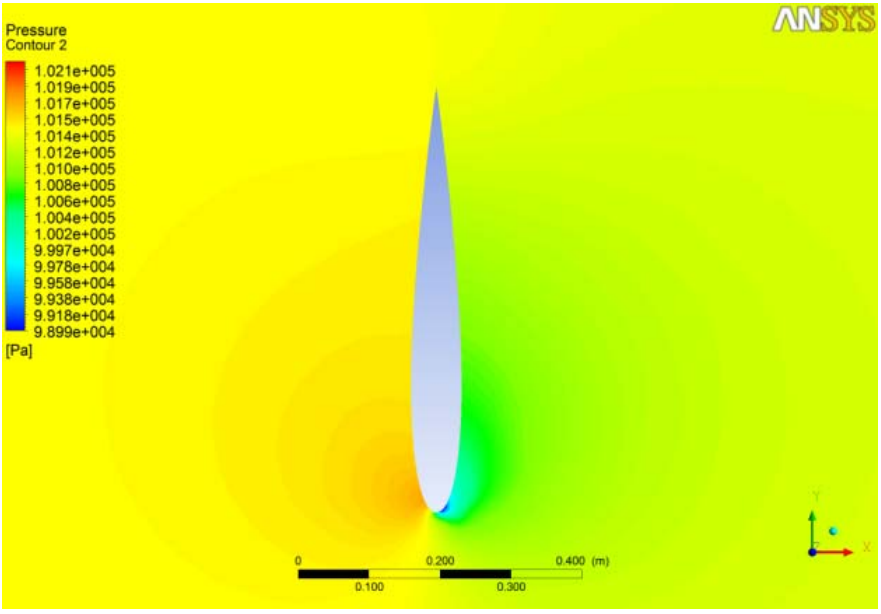

Fig. 3.6 VAWT - Pressure distribution around the blade located at θ=180º. Radius = 2.5 m. – Chord = 0.6 m. – NACA0012.

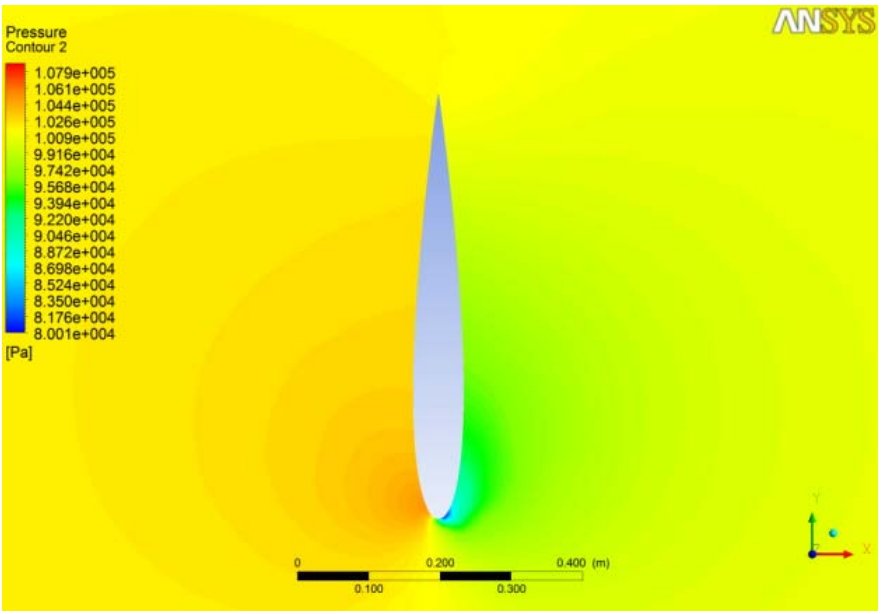

Fig. 3.7 VATT - Pressure distribution around the blade located at θ=180º. Radius = 2.5 m. – Chord = 0.6 m. – NACA0012.

Despite that the high and low pressure zones are distributed in a similar way for both turbines, the difference between maximum and minimum pressure (ΔP) is higher in the tidal turbine as seen in **Table 3.4**.

$$\Delta P = P_{\max} - P_{\min} \tag{3.4}$$

Therefore, the structure of the tidal turbine must be strengthened as it is dealing with stronger forces than the air turbine. Regarding the structural analysis of the turbine, a Fluid Structure Interaction (FSI) analysis is highly recommended to achieve a better understanding about the differences between wind and tidal turbines.

ΔP	
Air (VAWT)	**Water (VATT)**
3200 Pa	29000 Pa

Table 3.4 Maximum difference of pressure for VAWT and VATT.

After studying the velocity and pressure distribution for both turbines, **Fig. 3.8** and **Fig. 3.9** show the values of the efficiency C_p (see equation **(1.4)**) versus the tip speed ratio λ (see equation **(1.1)**) obtained through the simulations. In order to obtain the desired tip speed ratio, the rotational velocity of the turbine was changed in each simulation accordingly to its radius and the fluid velocity. **Table 3.5** also shows the time step values that provide a 5º mesh rotation as explained in section **3.2** about the time step independence study.

	VAWT		**VATT**	
TSR	**ω(rad/s)**	$\Delta t\|_{5^o}$ **(ms)**	**ω(rad/s)**	$\Delta t\|_{5^o}$ **(ms)**
1	4	21.82	0.4	218.17
1.5	6	14.54	0.6	145.44
2	8	10.91	0.8	109.08
2.5	10	8.73	1	87.27
3	12	7.27	1.2	72.72
3.5	14	6.23	1.4	62.33
4	16	5.45	1.6	54.54
4.5	18	4.85	1.8	48.48
5	20	4.36	2	43.63

Table 3.5 Time step values and turbine rotational velocity as a function of the tip speed ratio - Radius = 2.5m.

The simulation was made using two different blade chord values in order to see if this parameter affected the efficiency in a different way for wind or tidal

turbines. As it can be seen in **Fig. 3.9** no major differences were detected between the efficiency in water and air. As the blade chord is increased, the efficiency and the optimum tip speed ratio value are reduced as reported in [24]. A study about blade chord is presented in section **3.3.3.**

Only the positive values of the averaged moment coefficient were considered to calculate the power coefficient. As an efficiency value, the power coefficient must be always positive. The negative values obtained imply that the turbine is not capable to extract energy from the wind flow in these operating conditions, being necessary to supply the turbine with external energy in order to initiate its movement [25]. For reduced tip speed ratios it is usual to find negative moment coefficients that affect the self-starting behaviour of the turbine. In the next sections the effect of different turbine parameters over the turbine self-starting capabilities will be evaluated.

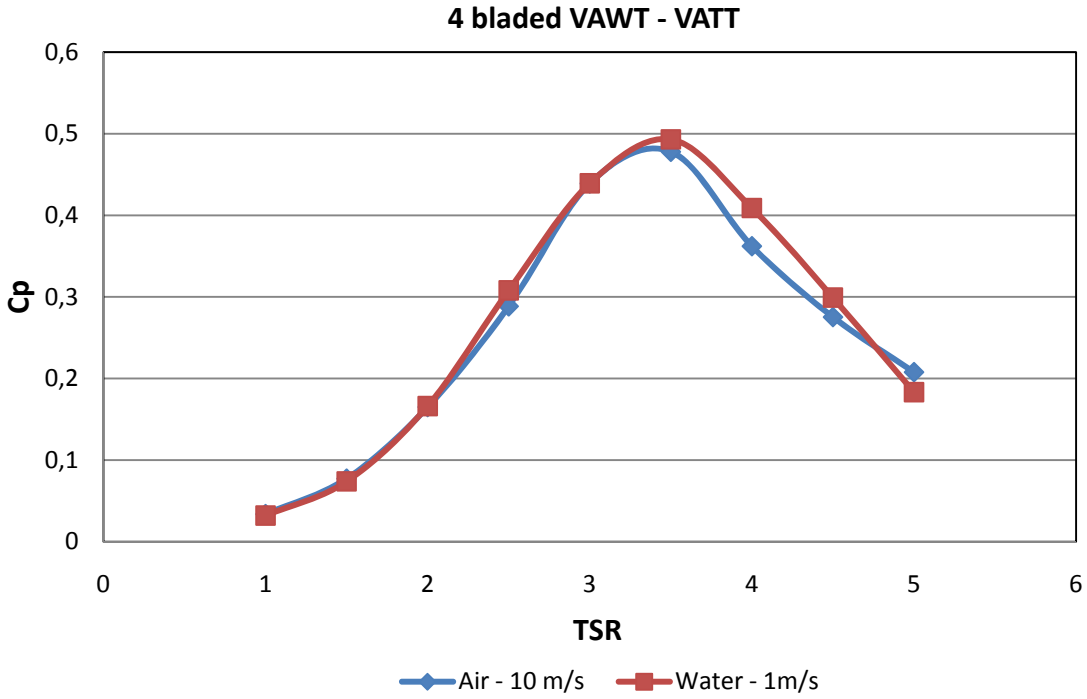

Fig. 3.8 Wind and tidal turbine efficiency comparison.
Radius = 2.5 m. - Chord = 0.3 m. - NACA0012.

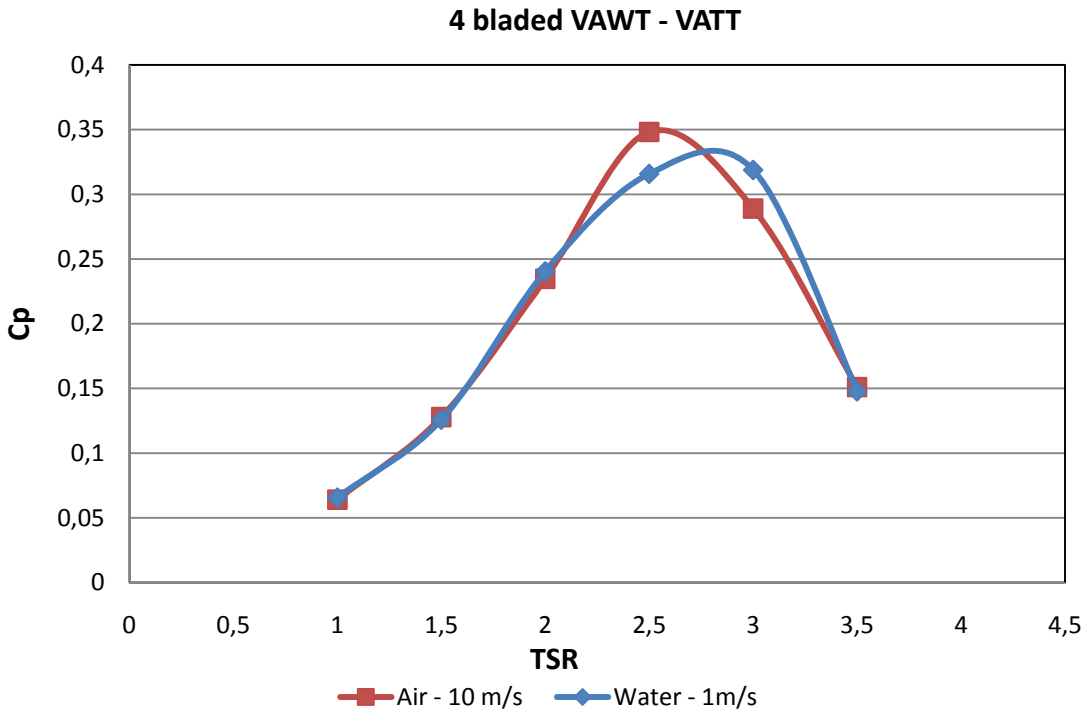

Fig. 3.9 Wind and tidal turbine efficiency comparison.
Radius = 2.5 m. - Chord = 0.6 m. - NACA0012.

From this point on, and due to similarity in the results between wind and tidal turbines in relation with their global efficiency, the rest of the simulations are based on a wind turbine.

3.3.2 Number of blades - Solidity

Up to this point, all the simulations consisted of a four bladed turbine. In order to study the effect of blade number over the turbine efficiency, a three bladed turbine is simulated with a radius of 2.5 meters. A blade chord value of 0.9 meters was used based on a NACA 0012 airfoil. It is usual to define the solidity parameter, which relates the number of blades of a turbine with its radius and blade chord. The expression of the solidity is detailed below:

$$\sigma = \frac{Nc}{R} \qquad \textbf{(3.5)}$$

Fig. 3.10 shows that the three bladed turbine provides a higher efficiency. This phenomenon is due to the fact that as the number of blades is increased, more turbulence is generated between blades, and the interference between detached vortices from the moving blades reduces turbine efficiency. Apart from the difference found in the efficiency, decreasing the number of blades increases the tip speed ratio at which maximum efficiency is reached. These effects regarding the number of blades have been described in [21] and [24].

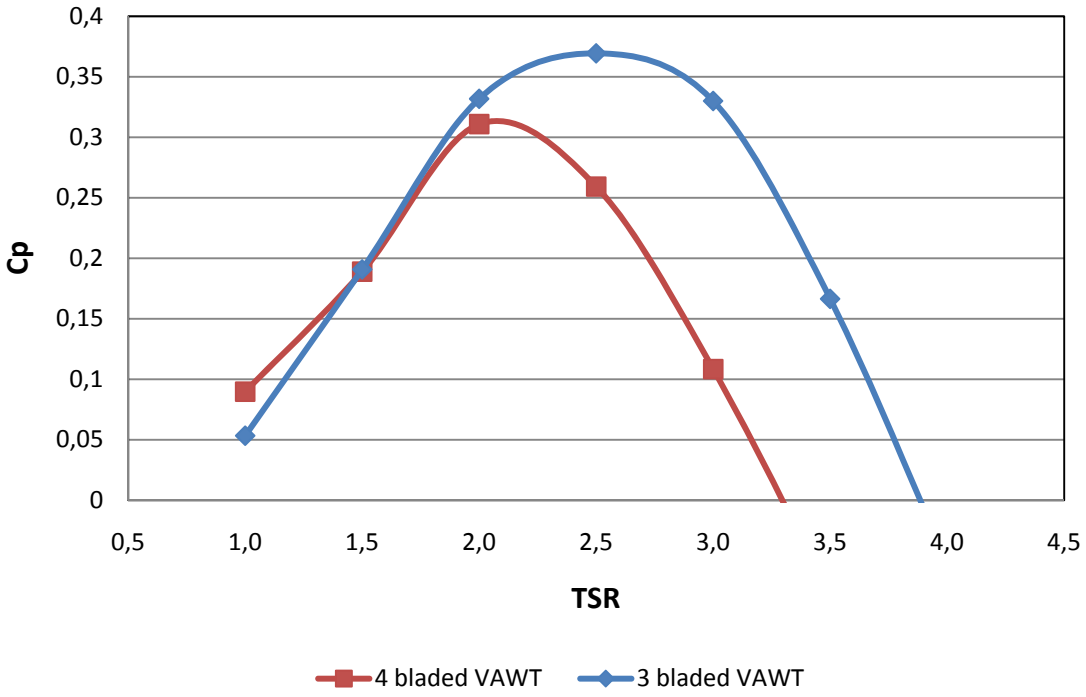

Fig. 3.10 Solidity effect in power coefficient.
Radius = 2.5 m. - Chord = 0.9 m. - NACA0012.

Table 3.6 shows the solidity values and maximum efficiency for each simulation:

# Blades	Solidity	λ_{opt}	C_{pMAX}
3	1.08	2.5	0.37
4	1.44	2	0.33

Table 3.6 Solidity values for the simulated turbines.

A comparison between 3, 4 and 5 bladed turbines is found in [14], where it is concluded that as the turbine solidity increases the maximum turbine efficiency and the optimum tip speed ratio are reduced.

Once the global efficiency of the turbines has been evaluated, **Fig. 3.11** shows the value of the moment coefficient for the three bladed turbine in one complete rotation as a function of the azimuth angle defined in **Fig. 3.3**. The contribution that the different blades have in the overall moment coefficient is studied, as well as the turbine moment coefficient. This value, as it was shown in equation **(3.1)**, is the sum of the moment for every blade of the turbine. Finally, note that the moment coefficient has a number of maximums in a complete revolution equal to the number blades of the turbine.

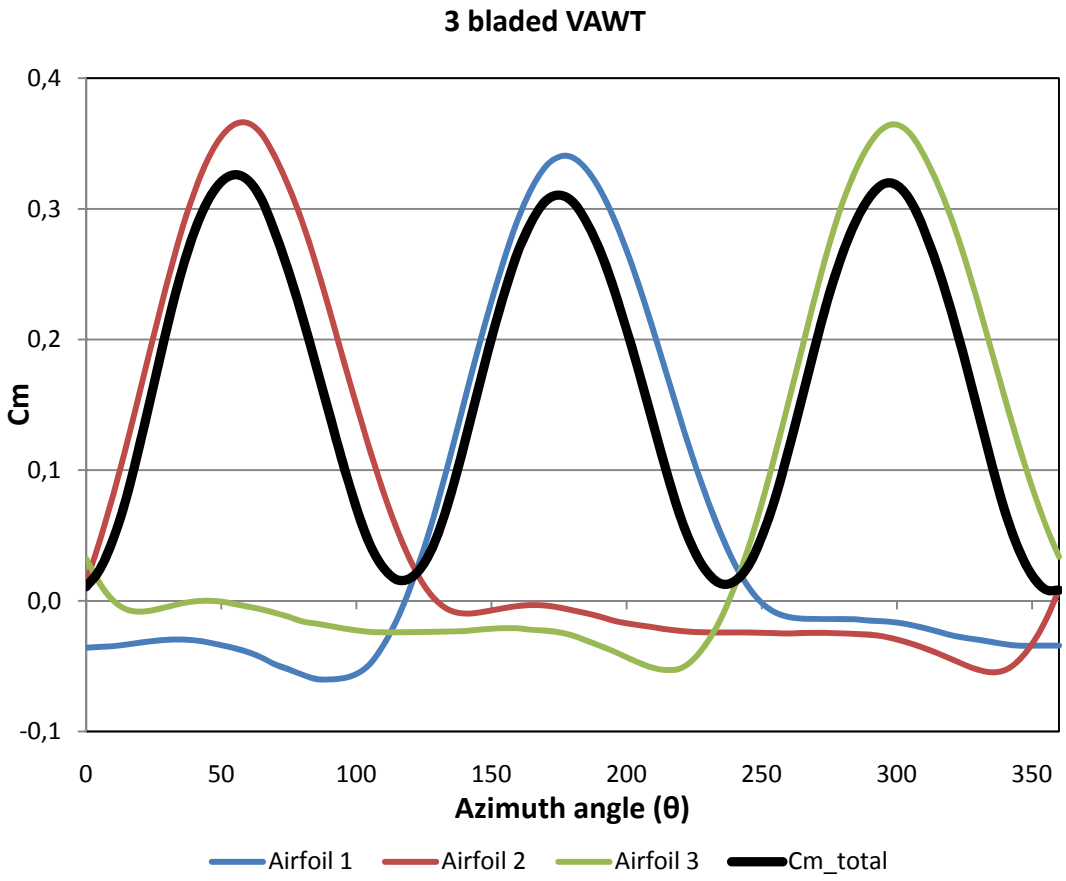

Fig. 3.11 Moment coefficient as a function of the azimuth angle. Radius = 2.5 m. - Chord = 0.9 m. - NACA0012.

Fig. 3.12 shows the moment coefficient of the turbine in a polar diagram as a function of the rotation of the turbine. The maximums of this function are located in three different angular positions at around 60º, 180º and 300º, which implies that the moment coefficient reaches a maximum value every time a blade is located at an azimuth position of 180º (see **Fig. 3.3**). This final assumption is demonstrated at **Fig. 3.13** where the moment coefficient for the blade 1 is plotted in a polar diagram.

Hence, when a turbine blade faces directly the free wind flow at a 180º azimuth position, it contributes with the maximum torque to the turbine. These results are very similar to the ones obtained in [23] and [26], where an azimuth analysis over a three bladed turbine is performed.

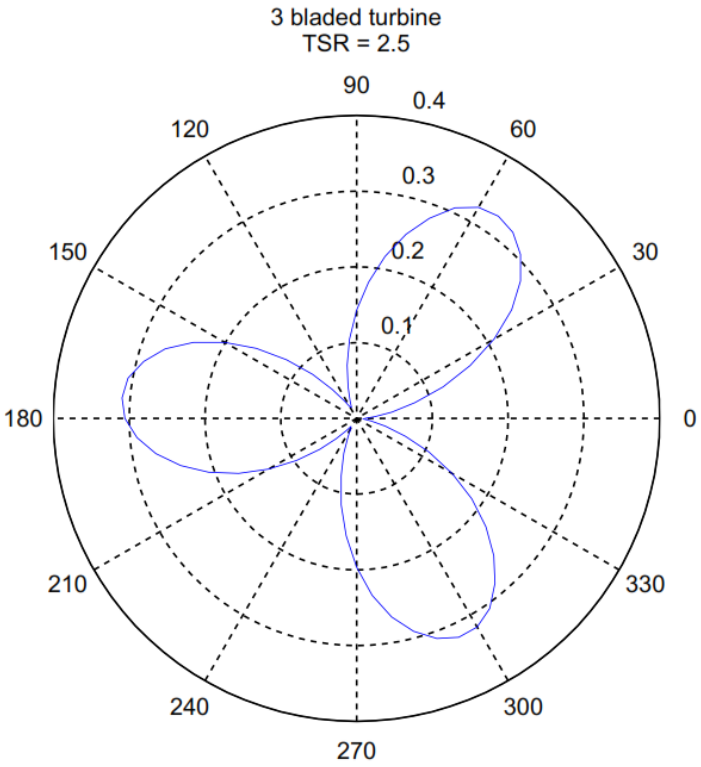

Fig. 3.12 Turbine moment coefficient as a function of the azimuth angle.

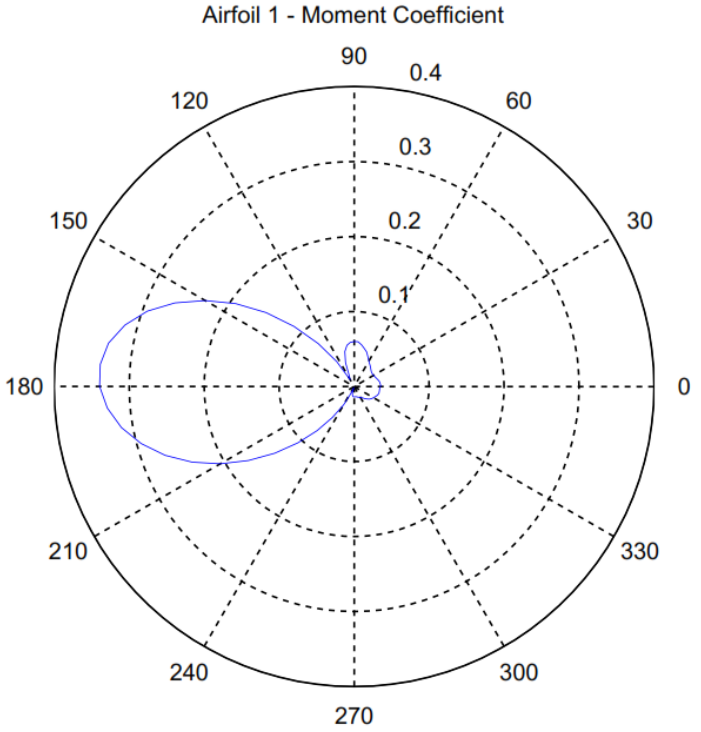

Fig. 3.13 Blade moment coefficient as a function of the azimuth angle.

3.3.3 Blade Chord effect

In this simulation the influence of the blade chord over the general performance of the turbine is studied. The simulation consisted of a four bladed turbine of a fixed radius of 2.5 meters and different values of blade chord: 0.3, 0.6 and 0.9 meters. **Fig. 3.14** shows the turbine efficiency as a function of the tip speed ratio for each different blade chord value simulated.

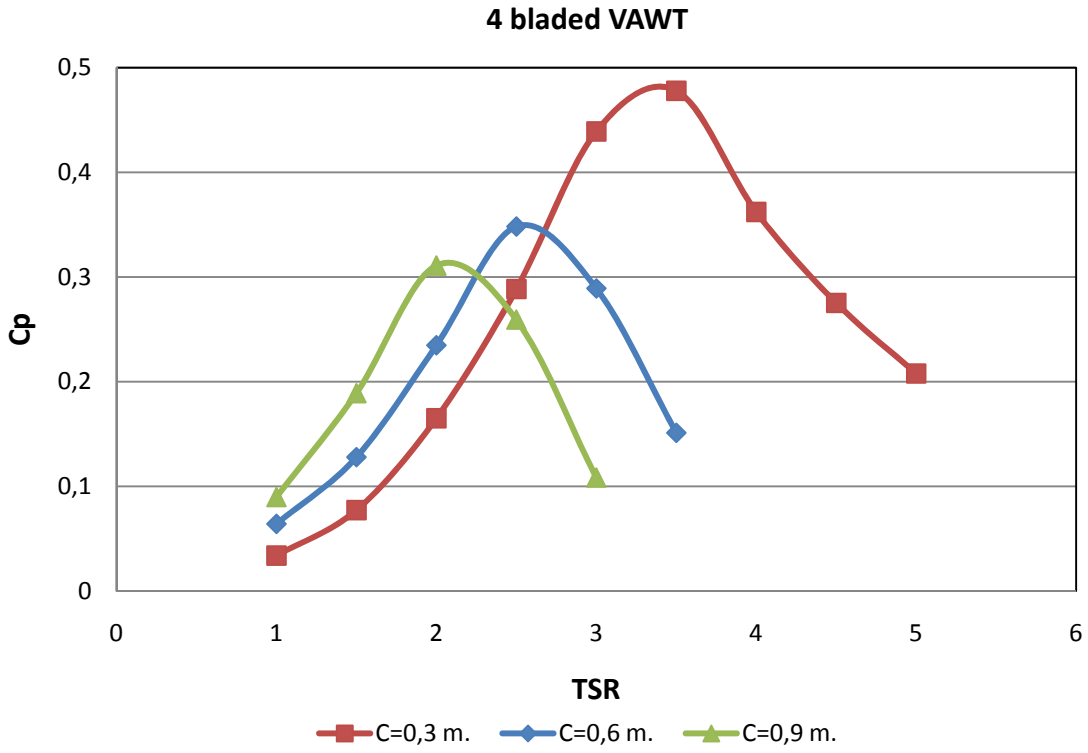

Fig. 3.14 Blade chord effect in power coefficient
Radius = 2.5 m. - NACA 0012.

From **Fig. 3.14** it is concluded that a bigger chord reduces the optimum tip speed ratio value where maximum efficiency is achieved, allowing the turbine to work at a lower wind velocity in an optimum way, which is a desirable feature of vertical axis turbines. In addition, as the blade chord is increased higher efficiency is achieved at low tip speed ratio values, improving the turbine self-starting capability. On the other hand, increasing the blade chord reduces the maximum efficiency of the turbine, as the maximum value of the power coefficient is reduced [24]. This behaviour was expected, because turbine solidity is proportional to the blade chord, and as it was explained in section **3.3.2** an increase in the solidity is related with a decrease in the overall turbine efficiency.

Therefore, a compromise must be reached between the maximum efficiency and the tip speed ratio value at which the maximum efficiency is achieved. For instance, in a zone with low wind velocities, it could be desirable to work with higher blade chords in order to maximize the time that the turbine works at optimum efficiency. However, if the average wind velocity of the zone is higher it

will be desirable to work with shorter chords to take the maximum benefit from the wind speeds.

3.3.4 Airfoil type effect

In this simulation different type of airfoils were tested. Due to the high amount of airfoils available, and in order to compare the results with the previous simulations, NACA symmetrical airfoils were used. Therefore, the only parameter that differs between the airfoils used in this simulation is the thickness. The NACA airfoils used were: NACA 0012, NACA 0015 and NACA 0021. As explained in section 2 these airfoils have a relation between thickness and chord equal to 12%, 15% and 21%.

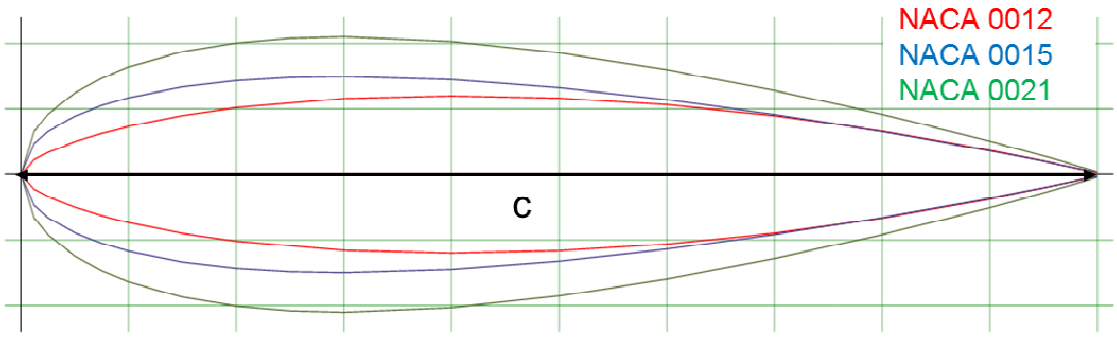

Fig. 3.15 NACA Airfoils used in the simulations.

The airfoils were used to generate a three bladed turbine with a blade chord of 0.9 meters. The effect of thickness variation in the global performance of the turbine is shown in **Fig. 3.16**. It can be seen that increasing the thickness of the airfoils improves the self-starting capability as well as the overall efficiency of the turbine. In addition, a slight advance of the point of maximum efficiency as the thickness airfoil increases is found. For instance, for the NACA 0021 airfoil the optimum tip speed ratio value is achieved at 1.5, while the NACA 0012 optimum tip speed ratio value is around 2.5. Moreover, as the airfoil thickness is increased the width of the efficiency curve around its maximum is increased, which implies that the turbine can work near its optimum efficiency zone in a higher range of tip speed ratio values.

Therefore, the results obtained in **Fig. 3.16** recommend the use of the thickest airfoil as it provides higher efficiency compared with the rest of the airfoils and also can withstand better with higher loads and forces. In addition, increasing the thickness of the blades widens the efficiency curve around its maximum, allowing the turbine to work with a wider range of fluid velocities near its optimum efficiency zone.

Finally, a study about the effect of blade thickness can be found at [24] and [26] showing a similar behaviour for the power coefficient curves found in this simulation.

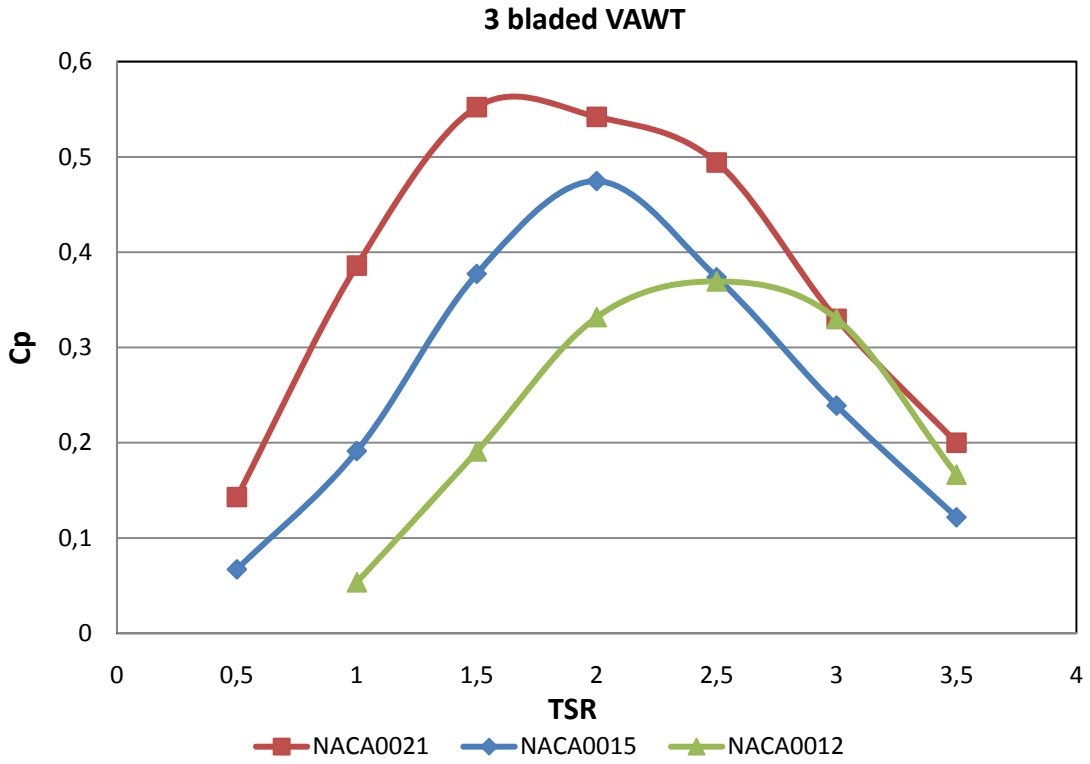

Fig. 3.16 Power coefficient as a function of the blade thickness. Radius = 2.5 m. – Chord = 0.9 m.

3.3.5 Turbine radius effect

This simulation studies the effect of the radius of the turbine over its efficiency. A bigger radius is related with a bigger torque, which at the same time provides a greater efficiency. In **Fig. 3.17** two vertical axis turbines of radius of 1 and 2.5 meters are compared using a NACA 0012 airfoil for the blades. Apart from the difference found regarding the power coefficient, as the radius of the turbine is increased the optimum tip speed ratio value increases.

In order to increase the efficiency of the turbine and considering the results obtained in the rest of the simulations, a suitable option is to increase the thickness of the airfoil used in the turbine of radius equal to 1 meter. Therefore, the simulation for the 1 meter radius turbine was repeated, but in this case a thicker NACA 0021 airfoil was used to generate the different blades. As it can be seen in **Fig. 3.17** the efficiency was dramatically increased, achieving values almost equal to the biggest turbine, while the global size of the turbine was not modified.

Attention must be paid to the range of useful tip speed ratio values for both turbines, as the smallest turbine has a good performance with lower tip speed ratios, while the 2.5 meters turbine has a better behaviour for higher tip speed ratio values. It can be concluded that prior to choose to size of the turbine, the desired tip speed ratio values or wind speed regime must be studied carefully.

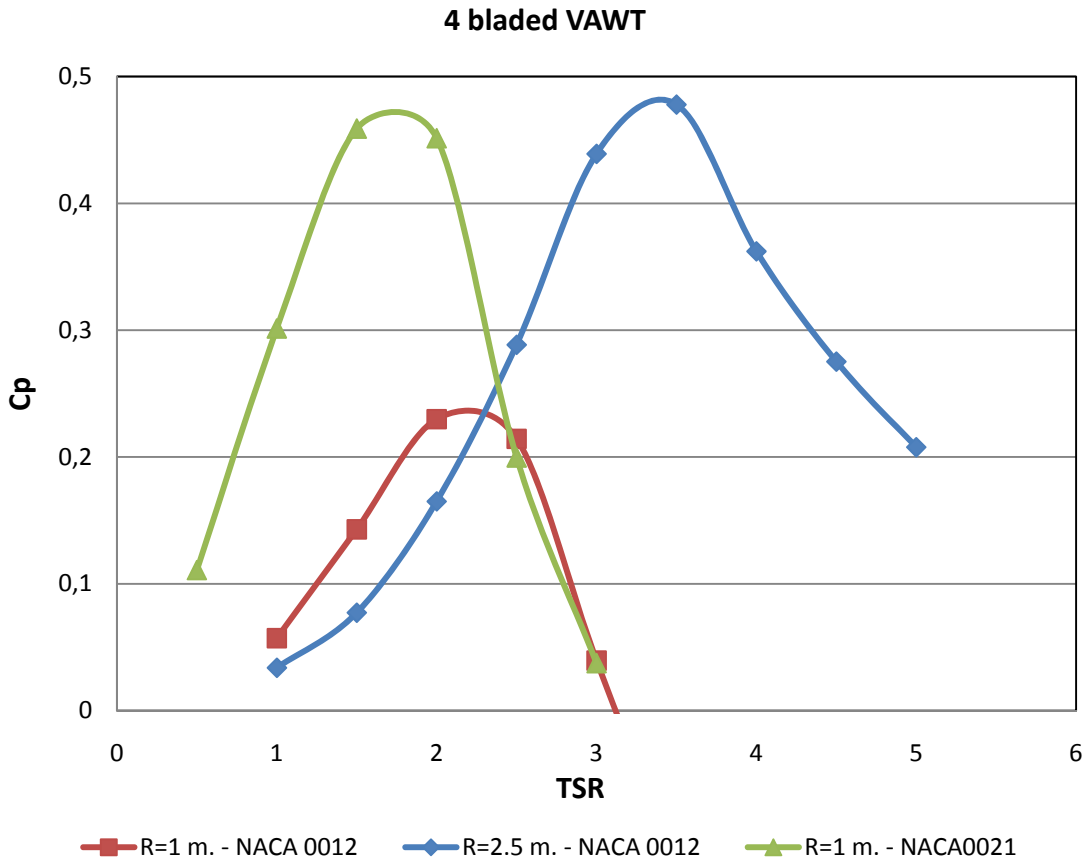

Fig. 3.17 Power coefficient as a function of turbine radius.
Chord = 0.3 m. - NACA0012.

CHAPTER 4. CONCLUSIONS AND FUTURE WORK

4.1 Conclusions

In this thesis the basics of a vertical axis turbine operation and its difference with horizontal axis turbines were detailed. Using CFD tools as *Fluent* allows simulating the designed 2D vertical axis turbines in different fluids such as air or water. Prior to initiate the simulations, a study about time and mesh independence was done in order to validate the results. After that, different simulations were done to study how different turbine parameters affect the overall performance. Then, in all simulations the moment coefficient of the turbine was calculated to obtain the power coefficient of the turbine for every value of tip speed ratio.

A comparison between wind and tidal turbines was conducted. The study led us to the conclusion that there is no substantial difference in the performance of the turbine from an aerodynamic point of view. Besides, the influence of the number of airfoils in the power coefficient was studied, where the three bladed turbine probed to be more efficient than the four bladed one. Indeed, the three bladed turbine maximum power coefficient was 0.37, whereas the value for the four bladed turbine was 0.31. Apart from that, the optimum tip speed ratio was reduced as the number of blades was increased.

A study about the moment coefficient as a function of the angle of rotation of the turbine was presented. As expected, the number of maximums of the turbine moment coefficient in a single rotation is related with the number of blades of the turbine. In addition a similar study over the blades demonstrated that the maximum torque was achieved when the blades passed through the 180º azimuth position, which was verified for both three and four bladed turbines. A blade reaches a 180º azimuth position when faces directly the free wind flow.

The influence of the airfoil was studied changing from the blade chord to the thickness of the airfoil. In the first case the shortest blade chord provided the highest efficiency. However, for low values of the tip speed ratio a bigger chord was suitable as it provided a higher efficiency, improving the self-starting capabilities of the turbine.

Moreover, different types of NACA symmetrical airfoils were tested over the same turbine, evaluating the influence of blades thickness. The simulations clearly showed that the thickest airfoil (NACA 0021) provided the highest efficiency, which was achieved for the lowest value of tip speed ratio compared with the rest of the airfoils. Besides, the higher efficiency obtained for low tip speed ratios, which as explained before improves the self-starting capabilities of the turbine, makes the NACA0021 airfoil as the most suitable option among the other two airfoils tested (NACA 0012 and NACA0015). Finally, NACA 0021 airfoil widens the efficiency curve, allowing the turbine to work near its optimum efficiency for a higher range of tip speed ratio values.

A simulation regarding the radius of the turbine was done, where the biggest turbine provided the highest efficiency. In order to increase the efficiency of the smallest turbine the original NACA 0012 airfoil was replaced with a thicker NACA 0021 as recommended by the previous results. As a result, the 1 meter radius turbine efficiency was increased reaching values similar to the ones provided by the biggest turbine. However, the optimum tip speed ratio zone was different for each turbine, as the biggest turbine has offers a good behaviour for higher tip speed ratio values, while the smallest turbine reaches its maximum efficiency for lower tip speed ratio values.

It can be concluded that the design and optimization of a vertical axis turbine has to consider all the parameters studied in this thesis together as they are related between them. In addition, factors such as the maximum size and wind regime must be taken into account.

4.2 Future Work

Note that because of the use of 2D simulations the efficiency values obtained through Ansys – Fluent are overestimated. Therefore, in a 3D simulation some effects like end tip vortices cannot be neglected and their effect would be a lower power coefficient.

The geometry of the turbine model used was very simple, as neither the supporting arms nor the central shaft of the turbine were considered. These parts of the turbine are supposed to worsen the efficiency values as they are merely structural elements which are not designed to generate lift. So a more realistic geometry in addition with a 3D CFD simulation is highly recommended to improve the accuracy and reliability of the results.

One of the problems of vertical axis turbines is their low efficiency at low tip speed ratio values which can affect their self-starting capabilities. As pointed by [20] and [25] the use of cambered airfoils can solve this issue. On the other hand cambered airfoils reduce the maximum efficiency of the turbine. Therefore, instead of using symmetrical airfoils, simulations based on cambered airfoils should be done.

From an aerodynamic point of view no substantial difference was found between wind and tidal turbines. However, a Fluid Structure Interaction (FSI) analysis should be done, as structural differences were arisen in the blade pressure distribution study. Therefore, tidal turbines are expected to have to withstand higher loads than air turbines.

BIBLIOGRAPHY

[1] Global Wind Energy Council, http://www.gwec.net

[2] R. Siegel, "Tidal Power: Pros and Cons," 2012. http://www.triplepundit.com/2012/06/tidal-power-pros-cons/

[3] Tidal Turbines, http://tidalturbines.wikispaces.com/Tidal+Current+Turbines

[4] Hans Bernhoff, Mats Leijon, Sandra Eriksson, "Evaluation of different turbine concepts for wind power," *Renewable and Sustainable Energy Reviews,* 2008.

[5] Wind Turbine, http://en.wikipedia.org/wiki/Wind_turbine

[6] http://technologygreenenergy.blogspot.com.es/2013/12/wind-turbine-generator-types.html

[7] Mahmoud Huleihil, Gedalya Mazor, "Wind Turbine Power: The Betz Limit and Beyond," vol. Chapter 1, 2012.

[8] Adam Ragheb, Magdi Ragheb, "Wind Turbines Theory - The Betz Equation and Optimal Rotor Tip Speed Ratio," University of Illinois at Urbana-Champaign, Talbot Laboratory, USA.

[9] Ansys, "Ansys Fluent Tutorial - Basic Steps for CFD Analysis using Ansys Fluent".

[10] Airfoil Tools - Airfoils Database, http://airfoiltools.com/airfoil/details?airfoil=naca0018-il

[11] NACA Airfoils, http://en.wikipedia.org/wiki/NACA_airfoil

[12] John D. Anderson, "Introduction to Flight," 6th ed., Mc Graw - Hill International Edition, 2008.

[13] Anibal Isidoro Carmona, "Origen de las fuerzas aerodinámicas," *Aerodinámica y actuaciones del avión*, Madrid, Thomson - Paraninfo, 2008.

[14] Stefano De Betta, Ernesto Benini, Marco Raciti Castelli, "Effect of Blade Number on a Straight-Bladed Vertical-Axis Darreius Wind Turbine," *World Academy of Science, Engineering and Technology,* vol. 61, 2012.

[15] Ansys, "Flows Using Sliding and Deforming Meshes".

[16] Ansys, "Boundary Conditions for Incompressible Flows".

[17] Ansys, "Setup and Solution of a Sliding Mesh Problem - Time-Periodic Solutions".

[18] Gallegos-Muñoz. A., Riesco Ávila J.Manuel, Uzarraga-Rodríguez N. Cristobal, "Numerical Analysis of a Rooftop Vertical Axis Wind Turbine," *Proceedings of the ASME 2011 5th International Conference on Energy Sustainability,* 7-10 August 2011.

[19] S. Lain, C. Osorio, "Simulation of Straight-Bladed Darrieus-type Cross Flow Turbine," *Journal of Scientific & Industrial Research,* 2010.

[20] Habtamu Beri, Yingxue Yao, "Effect of Camber Airfoil on Self Starting of Vertical Axis Wind Turbine," *Journal of Environmental Science and Technology,* pp. 302-312, 2011.

[21] Etesh Vaishnav, "An Investigation on the Aerodynamic Performance of a VAWT.," *Master of Science in Mechanical Engineering - Oklahoma State University,* 2010.

[22] Ansys, “Fluent Model Setup Tutorial”.

[23] Giulia Simoni Ernesto Benini, Marco Raciti Castelli, “Numerical Analysis of the Influence of Airfoil Asymmetry on VAWT Performance,” *World Academy of Science, Engineering and Technology,* pp. 312-321, 2012.

[24] Javier Castillo, "Small-scale Vertical Axis Wind Turbine Design", Tampere University of Applied Sciences, 2011.

[25] M.C. Claessens, "The Design and Testing of Airfoils for Application in Small Vertical Axis Wind Turbines", 2006.

[26] Yang Sun, Liang Zhang, “Airfoil Optimizaion of Vertical-axis Turbines Based on CFD Method,” *International Conference on Computer Modeling and Simulation*, 2010.

APPENDIX

The upper surface coordinates of the different NACA airfoils used in the simulations are listed in the next tables [10]:

NACA 0012

X coordinate	Y coordinate
0	0
0.0005839	0.0042603
0.0023342	0.0084289
0.0052468	0.0125011
0.0093149	0.0164706
0.0145291	0.02033
0.0208771	0.0240706
0.0283441	0.0276827
0.0369127	0.0311559
0.0465628	0.0344792
0.057272	0.0376414
0.0690152	0.040631
0.0817649	0.0434371
0.0954915	0.0460489
0.1101628	0.0484567
0.1257446	0.0506513
0.1422005	0.0526251
0.1594921	0.0543715
0.1775789	0.0558856
0.1964187	0.057164
0.2159676	0.0582048
0.2361799	0.0590081
0.2570083	0.0595755
0.2784042	0.0599102
0.3003177	0.0600172
0.3226976	0.0599028
0.3454915	0.0595747
0.3686463	0.0590419
0.3921079	0.0583145
0.4158215	0.0574033
0.4397317	0.05632
0.4637826	0.0550769
0.4879181	0.0536866
0.5120819	0.052162
0.5362174	0.0505161
0.5602683	0.0487619
0.5841786	0.0469124
0.6078921	0.0449802
0.6313537	0.0429778
0.6545085	0.0409174
0.6773025	0.0388109
0.6996823	0.03667
0.7215958	0.0345058
0.7429917	0.0323294
0.7638202	0.0301515
0.7840324	0.0279828
0.8035813	0.0258337
0.8224211	0.0237142
0.8405079	0.0216347
0.8577995	0.0196051
0.8742554	0.0176353
0.8898372	0.0157351
0.9045085	0.0139143
0.9182351	0.0121823
0.9309849	0.0105485
0.942728	0.0090217
0.9534372	0.0076108
0.9630873	0.0063238
0.9716559	0.0051685
0.9791229	0.0041519
0.9854709	0.0032804
0.990685	0.0025595
0.9947532	0.0019938
0.9976658	0.001587
0.9994161	0.0013419
1	0.00126

NACA 0015

X coordinate	Y coordinate
1	0.00158
0.95	0.01008
0.9	0.0181
0.8	0.03279
0.7	0.0458
0.6	0.05704
0.5	0.06617
0.4	0.07254
0.3	0.07502
0.25	0.07427
0.2	0.07172
0.15	0.06682
0.1	0.05853
0.075	0.0525
0.05	0.04443
0.025	0.03268
0.0125	0.02367
0	0

NACA 0021

X coordinate	Y coordinate
1	0.00221
0.95	0.01412
0.9	0.02534
0.8	0.04591
0.7	0.06412
0.6	0.07986
0.5	0.09265
0.4	0.10156
0.3	0.10504
0.25	0.10397
0.2	0.1004
0.15	0.09354
0.1	0.08195
0.075	0.0735
0.05	0.06221
0.025	0.04576
0.0125	0.03315
0	0